A Global Model of Linearized Atmospheric Perturbation: Model Description

By

Duane E. Stevens and Paul E. Ciesielski

Department of Atmospheric Science
Colorado State University
Fort Collins, Colorado

Colorado State University

Department of Atmospheric Science

Paper No. 377

A GLOBAL MODEL OF LINEARIZED ATMOSPHERIC PERTURBATIONS:

MODEL DESCRIPTION

Duane E. Stevens
and
Paul E. Ciesielski

Department of Atmospheric Science
Colorado State University
Fort Collins, CO   80524

February 1984

Abstract

This document provides a detailed discussion of the formulation and development of a global model of linearized perturbations. Although the model was originally designed for the purpose of studying tropical easterly waves, it has been built in a way that allows more general usage. The characteristics unique to this model and/or important for applications include:

(a) The specification of an "arbitrary" mean zonal flow which can depend on both latitude and height;

(b) Calculation of a mean meridional circulation which is dynamically consistent with the mean zonal flow (i.e., satisfies conservation of angular momentum, the balance approximation, the hydrostatic approximation, conservation of mass and energy);

(c) Vertical transport of momentum by the deep convective clouds in the tropics in both the mean and perturbation circulations;

(d) Spherical geometry;

(e) Coordinate stretching in both the vertical and latitudinal coordinates, which is represented in the coupled differential equations by finite differences;

(f) Very fine vertical grid resolution: experiments have been run with 31 points in the vertical; computer processing increases only linearly with the number of grid points in the vertical;

(g) Horizontal resolution of 15 to 20 points (square matrices with approximately five times the number of horizontal points must be inverted) at each vertical level;

(h) Very economic computation: the global response in a single zonal wavenumber is obtained with approximately 13 seconds of NCAR CRAY time.

ACKNOWLEDGMENTS

Table of Contents

1. Introduction

Recent observational studies have determined that vertical transport of vorticity and momentum by deep cumulus clouds is an important element in the dynamics of tropical weather systems with Doppler-shifted time scales on the order of a day or longer (i.e., with Doppler-shifted periods of at least six days). For example, Reed and Johnson (1974) found a substantial residual in the large-scale vorticity budget of western Pacific disturbances, which could be attributed to convective transports. Vorticity budget residuals were also found in the case of African wave disturbances by Shapiro (1978) and synoptic scale disturbances over the GATE ship array by Stevens (1979). Even though the moist convection had a much more complicated character over the Atlantic region than over the Pacific, the vorticity residuals could still be explained by cumulus transports (Shapiro, 1978, and Shapiro and Stevens, 1980). Shapiro and Stevens also found that the residuals in the momentum budgets, although subject to greater observational uncertainty, could also be ascribed to a large extent to cumulus transports.

Modeling studies have corroborated the importance of cumulus transports of momentum in tropical circulation system. Schneider and Lindzen (1977) and Schneider (1977) incorporated cloud momentum transport in calculations of the mean meridional circulations, or Hadley cell. Stevens et al. (1977) and Stevens and Lindzen (1978) showed that both the dynamic and the thermodynamic balances in tropical easterly waves are dramatically altered when cloud momentum transport is included. Mass (1979) found this process to be significant in his investigation of African wave instability. All of these studies used the Schneider-Lindzen (1976) parameterization for cumulus transport of momentum.

1

Although Stevens et al. (1977) demonstrated that the qualitative structure of tropical easterly waves changed significantly when cloud momentum transport was included, their simplifying assumptions precluded direct comparison with observed disturbances. In order to better understand the structure and dynamics of these weather systems, a model with a more realistic basic state is required. This document provides a detailed discussion of the formulation and development of such a three-dimensional model.

As in the earlier model, a zonally propagating heating function, representing release of latent heat in the convectively active part of the wave, is specified. The resulting circulation is calculated. For a consistent moisture budget, the specified diabatic heating should be approximately in phase with the calculated moisture convergence. A comparison of the phase and horizontal structure of the computed moisture convergence with the specified heating profile will provide a clue to the ability of these systems to propagate westward as neutral (i.e., non-growing and non-decaying) entities. The role of radiative perturbations in the waves, first considered by Albrecht and Cox (1975), can also be addressed. The heating function is assumed to be zonally periodic, of the form $\exp[i(s\lambda^*-\sigma t)]$, where s = zonal wavenumber, λ^* = longitude, and σ = frequency. We consider the linear response to this heating, since the observed disturbances propagate westward over the oceans, especially the Pacific, for many wavelengths without significant intensification or strong non-linear interactions.

The most important advance in model design is the explicit inclusion of a zonal ITCZ with associated vertical mass flux both on the cloud scale ($g\bar{M}_c$) and in the large-scale cloud environment ($\bar{\rho w}$). In the

Stevens $\underline{et}$ $\underline{al}$. study, $\bar{M}_c$ was taken to be horizontally uniform on the midlatitude beta plane, and the large-scale vertical velocity was neglected. These assumptions are only consistent with a basic state in uniform rotation, with no horizontal or vertical shear of the mean zonal wind. Since one of the goals of this investigation is to study the ramifications of a basic state zonal wind with both horizontal and vertical shear, the mass flux and associated transports of the meridional Hadley cell are necessary components of a consistent basic state with an ITCZ. Such a consistent basic state was the goal of the Hadley cell calculations by Schneider and Lindzen (1977) and Schneider (1977).

One of the goals of this research is to study the differences in structure and dynamics of tropical waves in the context of different mean wind profiles. Hence the well-documented waves in both the eastern Atlantic (Thompson $\underline{et}$ $\underline{al}$., 1979) and the western Pacific (Reed and Recker, 1971) can be considered. In spirit, the approach is similar to the early study of Holton (1971); however, we expect the results to be quite different because the dynamic effects of momentum transport by the convective elements in the ITCZ were not realized at the time, and therefore not considered.

It might be noted here that the instability analysis of Mass (1979) contained some elements of the present model, namely, zonal mean wind shear and cumulus friction. However, he ignored the zonally averaged mass flux in the clouds and consequently excluded any transports by the mean meridional circulation. This may be satisfactory over Africa, but certainly not over the oceans where the ITCZ is well-established. Also, because of the linearization assumption, he was forced to allow "negative precipiation" in his model. This drawback is eliminated when the

zonal mean cloud mass flux, and hence zonal mean precipitation, is explicitly incorporated as in the present model.

Although the model was originally designed for the purpose of studying tropical easterly waves, it has been built in a way that allows more general usage. Spherical geometry is assumed. The hydrostatic approximation is made from the beginning, so that a pressure-type independent variable is the vertical coordinate. User-specified coordinate stretching is included in the model design for both the latitudinal and vertical dimensions, which are represented in finite difference form; by specifying coordinate transformations through analytic functions and their derivatives, a user can focus his attention on a particular region of the globe. The earth's radius is assumed constant in the governing equations, and the gravitational acceleration is assumed constant in magnitude; for studying the lowest 100 km of the atmosphere, these assumptions are not severe limitations.

The model, which is semi-spectral, uses second-order finite difference representations in the latitudinal and vertical dimensions, while a single Fourier component is assumed in the zonal direction for the linearized perturbations. A single frequency for the perturbation is specified by the user in the time domain; this frequency may be real for neutrally-propagating waves, complex for unstably amplifying or stably decaying perturbations, or even zero for stationary waves. More generally, a calculation with longitudinal wavenumber s and temporal frequency σ can be considered a single component of a Fourier series in longitude and a Laplace transform in time.

In the present configuration, the pressure velocity is assumed to vanish at the lower boundary, assumed to be a surface of constant pressure. This boundary condition could be modified to represent the linear effect of flow over topography.

The model design requires vertical diffusion in the perturbation equations for horizontal momentum and temperature change. These diffusion terms can be relatively small.

As one of the primary purposes is to study the role of a Hadley cell as a basic state for the linearized perturbations, we specify the mean zonal wind and the mean cloud mass flux. Additionally, we use an empirically prescribed mean meridional circulation ($\bar{\psi}$) from which $\bar{v}$ and $\bar{w}$ are derived. As an alternative option, the user can "turn off" the mean meridional cell.

Finally, the model is designed for computational efficiency at very high vertical resolution. The computer time required is to a good approximation proportional to the number of vertical levels. At each vertical level a matrix inversion must be performed in which the matrix dimension is approximately five times the number of latitudinal grid points. A model run with 21 horizontal grid points and 31 vertical levels, uses approximately 13 seconds of CPU time on the NCAR CRAY-1 computer.

2. Full Primitive Equations and Model Parameters

For consistency all three components of the zonal mean circulation in the advection terms of the linearized perturbation equations are included. It is possible that some of the advective terms by the mean meridional cell $(\bar{v}, \bar{w})$ could be consistently scaled out for some problems, but in the interest of generality we have elected to leave them in. Following Holton (1975, p. 29) with slightly different notation, the (hydrostatic) primitive equations in log p coordinates on a sphere are written as follows:

U-Momentum

$$\frac{\partial u}{\partial t} + \frac{u}{a\cos\theta} \frac{\partial u}{\partial \lambda^*} + \frac{v}{a} \frac{\partial u}{\partial \theta} - \frac{uv}{a} \tan\theta + w \frac{\partial u}{\partial z} - fv + \frac{1}{a\cos\theta} \frac{\partial \Phi}{\partial \lambda^*}$$

$$= \frac{g}{p} \frac{\partial}{\partial z} \left[M_c(u-u_c) + \frac{\mu\dagger}{H} \frac{\partial u}{\partial z} \right] - \alpha_R u$$

(2.1)

V-Momentum

$$\frac{\partial v}{\partial t} + \frac{u}{a\cos\theta} \frac{\partial v}{\partial \lambda^*} + \frac{v}{a} \frac{\partial v}{\partial \theta} + w \frac{\partial v}{\partial z} + \frac{u^2}{a} \tan\theta + fu + \frac{1}{a} \frac{\partial \Phi}{\partial \theta}$$

$$= \frac{g}{p} \frac{\partial}{\partial z} \left[M_c(v-v_c) + \frac{\mu\dagger}{H} \frac{\partial v}{\partial z} \right] - \alpha_R v$$

(2.2)

Hydrostatic

$$\frac{\partial \Phi}{\partial z} = RT$$

(2.3)

Continuity

$$\frac{1}{\cos\theta} \frac{\partial u}{\partial \lambda^*} + \frac{1}{a} \frac{\partial v}{\partial \theta} - \frac{v}{a} \tan\theta + \frac{\partial w}{\partial z} - w = 0$$

(2.4)

Thermodynamic

$$\frac{\partial T}{\partial t} + \frac{u}{a\cos\theta}\frac{\partial T}{\partial \lambda^*} + \frac{v}{a}\frac{\partial T}{\partial \theta} + w\frac{\partial T}{\partial z} + w\kappa T = \frac{Q}{c_p} + \frac{g}{p}\frac{\partial}{\partial z}\frac{\hat{\mu}\dagger}{H}\frac{\partial T}{\partial z} - \alpha_N T \quad (2.5)$$

The vertical diffusion terms:

$$\frac{g}{p}\frac{\partial}{\partial z}\frac{\hat{\mu}\dagger}{H}\frac{\partial u}{\partial z}, \quad \frac{g}{p}\frac{\partial}{\partial z}\frac{\hat{\mu}\dagger}{H}\frac{\partial v}{\partial z}, \quad \text{and} \quad \frac{g}{p}\frac{\partial}{\partial z}\frac{\hat{\mu}\dagger}{H}\frac{\partial T}{\partial z}$$

are required by the numerical integration scheme. As noted by Stevens et al. (1977), vanishing of the mass flux M_c at the cloud-top level gives singular solutions of the inviscid equations which can be avoided by inclusion of small vertical diffusion terms. The independent variables for this system of equations are:

$\lambda^* \equiv$ longitude
$\theta \quad \equiv$ latitude
$t \quad \equiv$ time
$z \quad = \ln\left(\frac{p_o}{p}\right)$

The dependent variables for this system of equations are:

$u = a\cos\theta\,\dfrac{d\lambda^*}{dt} \equiv$ horizontal velocity component in λ^*-direction

$v = a\,\dfrac{d\theta}{dt} \equiv$ horizontal velocity component in θ-direction

$w = \dfrac{dz}{dt} \equiv$ vertical velocity component

$T \equiv$ temperature

$\Phi \equiv$ geopotential height

Other specified variables and constants are:

$f = 2\Omega\sin\theta \equiv$ coriolis parameter

$p = p_o e^{-z} \equiv$ pressure

$M_c \equiv$ cumulus mass flux

$Q \equiv$ diabatic heat source

$H = \dfrac{RT}{g} \equiv$ scale height

$g \equiv$ gravitational acceleration (9.81 ms^{-2})

$R \equiv$ gas constant for dry air (2.87×10^2 m^{2}s^{-2}°K^{-1})

$p_o \equiv$ surface pressure (10^5 N m^{-2})

$\Omega \equiv$ angular speed of rotation of earth (7.292×10^{-5} s^{-1})

$a \equiv$ mean radius of earth (6.37×10^6 m)

$z_c \equiv$ height of cloud base

$u_c = u(z_c) \equiv$ u-component of wind at cloud base

$v_c = v(z_c) \equiv$ v-component of wind at cloud base

$\alpha_R \equiv$ Rayleigh friction ($2\Omega \times$ DISWIND), where DISWIND is the non-dimensional dissipation coefficient of the horizontal wind

$\alpha_N \equiv$ Newtonian cooling ($2\Omega \times$ DISTEMP), where DISTEMP is the non-dimensional dissipation coefficient of temperature

$c_p \equiv$ specific heat of air at constant pressure (1004 m^{2}s^{-2}°K^{-1})

$\kappa = R/c_p$

$\mu\dagger \equiv$ dynamic coefficient of viscosity

$\hat{\mu}\dagger \equiv$ dynamic coefficient of thermal diffusion

Other constants used in this model but not explicitly appearing in equations 2.1-2.5 are listed below for the readers convenience.

$\pi =$ Acos (-1.)

$\sigma \equiv$ angular frequency (- Ω/PERIOD)

$s \equiv$ longitudinal wavenumber

$c \equiv$ phase speed ($\sigma \cdot a \cdot \cos\theta / s$)

$T_o \equiv$ surface temperature (300°K)

$U_o \equiv$ horizontal wind scale used in non-dimensionalization (10ms^{-1})

$V_o \equiv$ gustiness factor (8 ms^{-1})

CD $\equiv$ surface drag coefficient ($[1.0 + 0.07 \times V_o] \times$ 1E-3)

ST $\equiv$ static stability (878 m)

$\Gamma_1 = \frac{g \times ST}{R}$ (30.01°K)

IZ = number of points in z-direction

IY = number of points in θ-direction

ZT = z(IZ) $\equiv$ value of z at top of model

ZTROP $\equiv$ value of z at tropopause

3. Linearized Equations

Using the perturbation method all variables are expanded into two parts, a basic state which is assumed to be independent of time and longitude and a perturbation which is a local deviation of the field from the basic state. This expansion is shown below.

$$
\begin{aligned}
u(\lambda^*,\theta,z,t) &= \bar{u}(\theta,z) + \\
v(\lambda^*,\theta,z,t) &= \bar{v}(\theta,z) + \\
w(\lambda^*,\theta,z,t) &= \bar{w}(\theta,z) + \\
\Phi(\lambda^*,\theta,z,t) &= \bar{\Phi}(\theta,z) + \\
T(\lambda^*,\theta,z,t) &= \bar{T}(\theta,z) + \\
M_c(\lambda^*,\theta,z,t) &= \bar{M}_c(\theta,z) + \\
u_c(\lambda^*,\theta,z,t) &= \bar{u}_c(\theta,z) + \\
v_c(\lambda^*,\theta,z,t) &= \bar{v}_c(\theta,z) + \\
Q(\lambda^*,\theta,z,t) &= \bar{Q}(\theta,z) +
\end{aligned}
\left.
\begin{aligned}
u'(\theta,z) \\
v'(\theta,z) \\
w'(\theta,z) \\
\Phi'(\theta,z) \\
T'(\theta,z) \\
M'_c(\theta,z) \\
u'_c(\theta,z) \\
v'_c(\theta,z) \\
Q'(\theta,z)
\end{aligned}
\right\} \times e^{i(s\lambda^* - \sigma t)}
$$

where

$$(\bar{\ }) \equiv \text{basic state}$$

$$(\tilde{\ }) = (\ )' e^{i(s\lambda - \sigma t)} \equiv \text{perturbation from basic state}$$

To illustrate how Eqs. 2.1-2.5 are linearized we have shown below how this method works for the u-component of advection term in the u-momentum equation. Upon expansion:

$$
\frac{u}{a\cos\theta}\frac{\partial u}{\partial \lambda^*} = \frac{1}{a\cos\theta}\left(\bar{u}\frac{\partial \bar{u}}{\partial \lambda^*} + \bar{u}\frac{\partial \tilde{u}}{\partial \lambda^*} + \tilde{u}\frac{\partial \bar{u}}{\partial \lambda^*} + \tilde{u}\frac{\partial \tilde{u}}{\partial \lambda^*}\right)
\tag{3.1}
$$

The assumption is made here that the basic state variables must themselves satisfy the governing equations so that the first term on the right hand side of (3.1) will cancel out with the other terms of the basic state equation. Secondly, we assume that terms which involve

10

products of perturbation variables (e.g., last term on R.H.S. of (3.1)) can be neglected since $()' << (\bar{\ })$. In addition,

$$\frac{\partial(\tilde{\ })}{\partial\lambda^*} = is(\tilde{\ })$$

and

$$\frac{\partial(\tilde{\ })}{\partial t} = - i\sigma(\tilde{\ })$$

so that

$$\frac{\partial u'}{\partial\lambda^*} = \frac{\partial}{\partial\lambda^*}(u'(\theta,z)e^{i(s\lambda^*-\sigma t)}) = is[u'(\theta,z)e^{i(s\lambda^*-\sigma t)}] = is\tilde{u}$$

Therefore Eq. 3.1 can be simplied to:

$$\frac{u}{a\cos\theta}\frac{\partial u}{\partial\lambda^*} = \frac{\bar{u}\ isu'}{a\cos\theta} + \frac{u'}{a\cos\theta}\frac{\partial\bar{u}}{\partial\lambda^*}$$

By using this method to linearize the other terms in Eqs. (2.1-2.5), our system of equations now in their linearized perturbation form are given as follows:

U-Momentum

$$[-i\sigma + \frac{is\bar{u}}{a\cos\theta} + \alpha_R + \frac{\bar{v}}{a}\frac{\partial}{\partial\theta} + \bar{w}\frac{\partial}{\partial z} - \frac{\bar{v}}{a}\tan\theta - \frac{g}{p}\frac{\partial}{\partial z}\overline{M_c} - \frac{g}{p}\frac{\partial}{\partial z}\frac{\mu\dagger}{H}\frac{\partial}{\partial z}]u'$$

$$+ [\frac{1}{a}\frac{\partial\bar{u}}{\partial\theta} - \frac{\bar{u}}{a}\tan\theta - f]v' + [\frac{\partial\bar{u}}{\partial z}]w' \qquad\qquad (3.2)$$

$$+ [\frac{is}{a\cos\theta}]\phi' = - \frac{g}{p}\frac{\partial}{\partial z}[\overline{M_c}\ u'_c + M'_c\ (\bar{u}_c - \bar{u})]$$

V-Momentum

$$[\frac{2\bar{u}}{a}\tan\theta + f]u'$$

$$\qquad\qquad (3.3)$$

$$+ [-i\sigma + is\frac{\bar{u}}{a\cos\theta} + \alpha_R + \frac{\bar{v}}{a}\frac{\partial}{\partial\theta} + \bar{w}\frac{\partial}{\partial z} + \frac{1}{a}\frac{\partial\bar{v}}{\partial\theta} - \frac{g}{p}\frac{\partial}{\partial z}\overline{M_c} - \frac{g}{p}\frac{\partial}{\partial z}\frac{\mu\dagger}{H}\frac{\partial}{\partial z}]v'$$

$$+ [\frac{\partial\bar{v}}{\partial z}]w' + [\frac{1}{a}\frac{\partial}{\partial\theta}]\Phi' = -\frac{g}{p}\frac{\partial}{\partial z}[\overline{M_c}v_c' + M_c'(\bar{v}_c - \bar{v})]$$

Hydrostatic Approximation

$$[\frac{\partial}{\partial z}]\Phi' + [-R]T' = 0 \qquad\qquad (3.4)$$

Continuity

$$[\frac{is}{a\cos\theta}]u' + [\frac{1}{a}\frac{\partial}{\partial\theta} - \frac{\tan\theta}{a}]v' + [\frac{\partial}{\partial z} - 1]w' = 0 \qquad\qquad (3.5)$$

Thermodynamic

$$[\frac{1}{a}\frac{\partial\bar{T}}{\partial\theta}]v' + [\frac{\partial\bar{T}}{\partial z} + \bar{T}\kappa]w'$$

$$+ [-i\sigma + \frac{\bar{u}}{a}\frac{is}{a\cos\theta} + \alpha_N + \frac{\bar{v}}{a}\frac{\partial}{\partial\theta} + \bar{w}\frac{\partial}{\partial z} + \bar{w}\kappa - \frac{g}{p}\frac{\partial}{\partial z}\frac{\hat{u}\dagger}{H}\frac{\partial}{\partial z}]T' \qquad (3.6)$$

$$= \frac{Q'}{c_p}$$

4. Coordinate Stretching

To allow us the capability of stretching the coordinates in certain regions of the model's domain, (e.g., to increase resolution in regions of interesting phenomena) we transformed the vertical (z) and horizontal (θ) coordinates of the model into the independent variables $\lambda(z)$ and $\eta(y)$, respectively. By defining:

$\eta = \eta(y)$ is the stretched latitudinal coordinate

$y = a\theta$ is the latitudinal distance from the equator

$$\eta' = \frac{d\eta}{dy}$$

$$\frac{\partial}{\partial\theta} = a\eta' \frac{\partial}{\partial\eta}$$

$\lambda = \lambda(z)$ is the stretched vertical coordinate

$$\lambda' = \frac{\partial\lambda}{\partial z}$$

$$\frac{\partial}{\partial z} = \lambda' \frac{\partial}{\partial\lambda}$$

$$k = \frac{s}{a\cos\theta}$$

$\nu = \dfrac{\mu^\dagger}{\underline{\rho}}$ is the kinematic coefficient of viscosity

$\hat{\nu} = \dfrac{\hat{\mu}^\dagger}{\underline{\rho}}$ is the kinematic coefficient of thermal diffusion

$$\bar{p} = \bar{\rho}R\bar{T} = \bar{\rho}g\bar{H}$$

Eqs. 3.2-3.6 can then be written as:

U-MOMENTUM $\qquad$ (4.1)

$$[-i\sigma+ik\bar{u}+\alpha_R-\frac{\bar{v}}{a}\tan\theta + \bar{v}\eta'\frac{\partial}{\partial\eta} + \bar{w}\lambda'\frac{\partial}{\partial\lambda} - \frac{g}{p}\lambda'\frac{\partial}{\partial\lambda}\bar{M}_c - \frac{g}{p}\lambda'\frac{\partial}{\partial\lambda}\frac{p\nu}{gH^2}\lambda'\frac{\partial}{\partial\lambda}]u'$$

$$+ [\eta'\frac{\partial\bar{u}}{\partial\eta} - \frac{\bar{u}}{a}\tan\theta - f]v' + [\lambda'\frac{\partial\bar{u}}{\partial\lambda}]w'$$

$$+ [ik]\Phi' + \frac{g}{p}\lambda'\frac{\partial}{\partial\lambda}(\bar{M}_c u_c') = -\frac{g}{p}\lambda'\frac{\partial}{\partial\lambda}[M_c'(\bar{u}_c - \bar{u})]$$

V-MOMENTUM $\qquad$ (4.2)

$$[\frac{2\bar{u}}{a}\tan\theta + f]u'$$

$$+ [-i\sigma+ik\bar{u}+\alpha_R+\eta'\frac{\partial\bar{v}}{\partial\eta} + \bar{v}\eta'\frac{\partial}{\partial\eta} + \bar{w}\lambda'\frac{\partial}{\partial\lambda} - \frac{g}{p}\lambda'\frac{\partial}{\partial\lambda}\bar{M}_c - \frac{g}{p}\lambda'\frac{\partial}{\partial\lambda}\frac{p\nu}{gH^2}\lambda'\frac{\partial}{\partial\lambda}]v'$$

$$+ [\lambda'\frac{\partial\bar{v}}{\partial\lambda}]w'+[\eta'\frac{\partial}{\partial\eta}]\Phi'+ \frac{g}{p}\lambda'\frac{\partial}{\partial\lambda}(\bar{M}_c v_c') = -\frac{g}{p}\lambda'\frac{\partial}{\partial\lambda}[M_c'(\bar{v}_c - \bar{v})]$$

HYDROSTATIC APPROXIMATION $\qquad$ (4.3)

$$[\lambda'\frac{\partial}{\partial\lambda}]\Phi' + [-R]T' = 0$$

CONTINUITY $\qquad$ (4.4)

$$[ik]u' + [\eta'\frac{\partial}{\partial\eta} - \frac{\tan\theta}{a}]v' + [\lambda'\frac{\partial}{\partial\lambda} - 1]w' = 0$$

THERMODYNAMIC $\qquad$ (4.5)

$$[\eta'\frac{\partial\bar{T}}{\partial\eta}]v' + [\lambda'\frac{\partial\bar{T}}{\partial\lambda} + \bar{T}\kappa]w'$$

$$+ [-i\sigma+ik\bar{u}+\alpha_N+\bar{v}\eta'\frac{\partial}{\partial\eta} + \bar{w}\lambda'\frac{\partial}{\partial z} + \bar{w}\kappa - \frac{g}{p}\lambda'\frac{\partial}{\partial\lambda}\frac{p\hat{\nu}}{gH^2}\lambda'\frac{\partial}{\partial\lambda}]T'$$

$$= \frac{Q'}{c_p}$$

5. Flux Form of Equations

To satisfy general conservation properties in finite difference form and to place the vertical advection and cumulus friction terms in the same form, we have chosen at this time to rewrite the equations in flux form. The advection operator in the meridional plane becomes a flux operator when combined with the continuity equation (15.4) for the basic state:

$$\bar{v}\eta' \frac{\partial}{\partial \eta} + \bar{w}\lambda' \frac{\partial}{\partial \lambda} \equiv \frac{\eta'}{\cos\theta} \frac{\partial}{\partial \eta} \bar{v}\cos\theta + \frac{\lambda'}{(p/p_o)} \frac{\partial}{\partial \lambda} \frac{p}{p_o} \bar{w}$$

Using this identity the equations in flux form become:

U-MOMENTUM   (5.1)

$$(-i\sigma + ik\bar{u} + \alpha_R - \frac{\bar{v}}{a}\tan\theta)u' + \frac{\eta'}{\cos\theta} \frac{\partial}{\partial \eta} (\bar{v}\cos\theta u') + (\frac{\lambda'}{p/p_o}) \frac{\partial}{\partial \lambda} [(\frac{p}{p_o}\bar{w} - \frac{g\bar{M}_c}{p_o})u']$$

$$-(\frac{\lambda'}{p/p_o}) \frac{\partial}{\partial \lambda} \frac{p}{p_o} \frac{\nu}{H^2} \lambda' \frac{\partial u'}{\partial \lambda} + (\eta' \frac{\partial \bar{u}}{\partial \eta} - \frac{\bar{u}}{a}\tan\theta - f)v' + (\lambda' \frac{\partial \bar{u}}{\partial \lambda})w' + (ik)\Phi'$$

$$+ (\frac{\lambda'}{p/p_o}) \frac{\partial}{\partial \lambda} (\frac{g\bar{M}_c}{p_o})u'_c = - (\frac{\lambda'}{p/p_o}) \frac{\partial}{\partial \lambda} [\frac{g\bar{M}_c}{p_o} (\bar{u}_c - \bar{u})]$$

V-MOMEUNTUM   (5.2)

$$(\frac{2\bar{u}}{a}\tan\theta + f)u' + (-i\sigma + ik\bar{u} + \alpha_R + \eta' \frac{\partial \bar{v}}{\partial \eta})v' + \frac{\eta'}{\cos\theta} \frac{\partial}{\partial \eta} (\bar{v}\cos\theta v')$$

$$+ \frac{\lambda'}{p/p_o} \frac{\partial}{\partial \lambda} [(\frac{p}{p_o}\bar{w} - \frac{g\bar{M}_c}{p_o})v'] - (\frac{\lambda'}{p/p_o}) \frac{\partial}{\partial \lambda} \frac{p}{p_o} \frac{\nu}{H^2} \lambda' \frac{\partial v'}{\partial \lambda} + (\lambda' \frac{\partial \bar{v}}{\partial \lambda})w'$$

$$+ \eta' \frac{\partial \Phi'}{\partial \eta} + \frac{\lambda'}{p/p_o} \frac{\partial}{\partial \lambda} (\frac{g\bar{M}_c}{p_o})v'_c = - (\frac{\lambda'}{p/p_o}) \frac{\partial}{\partial \lambda} [\frac{g\bar{M}'_c}{p_o} (\bar{v}_c - \bar{v})]$$

15

HYDROSTATIC (5.3)

$$[\lambda \frac{\partial}{\partial \lambda}]\Phi' + [-R]T'$$

CONTINUITY (5.4)

$$(ik)u' + \frac{\eta'}{\cos\theta} \frac{\partial}{\partial \eta} (v'\cos\theta) + (\frac{\lambda'}{p/p_o}) \frac{\partial}{\partial \lambda} (\frac{p}{p_o} w') = 0$$

THERMODYNAMIC (5.5)

$$(\eta' \frac{\partial \bar{T}}{\partial \eta})v' + (\lambda' \frac{\partial \bar{T}}{\partial \lambda} + \bar{T}\kappa)w' + (-i\sigma+ik\bar{u} + \alpha_N)T'$$

$$\bar{v} \eta' \frac{\partial T'}{\partial \eta} + e^{-\kappa z} \bar{w} \lambda' \frac{\partial}{\partial \lambda} (e^{\kappa z}T') - \frac{\lambda'}{p/p_o} \frac{\partial}{\partial \lambda} \frac{p}{p_o} \frac{\hat{v}}{H^2} \lambda' \frac{\partial T'}{\partial \lambda} = \frac{Q'}{c_p}$$

6. Non-Dimensional Form of Equations

It is now convenient to non-dimensionalize the equations so that the solutions and the coefficients of the terms in the equations are $O(1)$. The following variables in our system of equations are non-dimensionalized as follows:

$$f \text{ by } 2\Omega$$

$$\sigma \text{ by } U_o/L$$

$$t \text{ by } L/U_o$$

$$x,y \text{ by } L = a/s' \text{ where } s' = \begin{cases} 1 \text{ for } s = 0 \\ s \text{ for } s \neq 0 \end{cases}$$

$$z \text{ by } 1$$

$$\bar{u}, u', \bar{v}, v' \text{ by } U_o$$

$$\bar{w}, \frac{g\bar{M}_c}{P_o}, \frac{g\bar{M}'_c}{P_o}, w' \text{ by } \frac{U_o}{L}$$

$$\Phi' \text{ by } 2\Omega U_o L$$

$$T' \text{ by } 2\Omega U_o L/R$$

To simplify the form of the non-dimensional equations we define the the following quantities

$$R_o \equiv U_o/2\Omega L \quad \text{is the Rossby number}$$

$$R_i = \frac{R\Gamma_1}{U_o^2} \quad \text{is the Richardson number}$$

$$Fr = \frac{U_o^2}{R\Gamma_1} = Ro^2\varepsilon = Ri^{-1} \quad \text{is the Froude number}$$

$$\xi \equiv p/p_o = e^{-z} \quad \text{is non-dimensional pressure}$$

$$E_o \equiv \nu/2\Omega H^2 = E_o(\eta,\lambda)$$

$$\hat{E}_o \equiv \hat{\nu}/2\Omega H^2 = \hat{E}_o(\eta,\lambda)$$

17

$$\varepsilon = \frac{4\Omega^2 L^2}{R\Gamma_1} = \frac{L^2}{a^2}\frac{4\Omega^2 a^2}{R\Gamma_1} = \left(\frac{2\Omega L}{U_o}\right)^2 \frac{U_o^2}{R\Gamma_1} = R_o^{-2}Fr = R_o^{-2}R_i^{-1}$$

$$\delta = L/a = 1/s'$$

$$f^* = f/2\Omega$$

$$\sigma^* = \frac{\sigma}{U_o/L}$$

$$\bar{u}^*, \ u'^*, \ \bar{v}^*, \ v'^* = \frac{\bar{u}}{U_o}, \ \frac{u'}{U_o}, \ \frac{\bar{v}}{U_o}, \ \frac{v'}{U_o}$$

$$\bar{w}^*, \ w'^* = \frac{\bar{w}}{U_o/L}, \ \frac{w'}{U_o/L}$$

$$\bar{M}_c^*, \ M_c'^* = \frac{g\bar{M}_c}{p_o U_o/L}, \ \frac{g\bar{M}_c'}{p_o U_o/L}$$

$$\Phi'^* = \frac{\Phi'}{2\Omega L U_o}$$

$$T'^* = \frac{T'}{2\Omega L U_o/R}$$

$$Q'^* = \frac{L}{U_o \Gamma_1} \ \frac{Q'}{c_p} \quad , \text{ where } \Gamma_1 \text{ is a typical stability}$$

where the ()* represents a non-dimensional quantity. Using these definitions and notation the linearized system of equations in flux form are non-dimensionalized as follows. The u momentum equation is multiplied by $(1/2\Omega U_o)$, and thus can be written as

$$\frac{U_o}{2\Omega L}\left(\frac{-i\sigma + i\dfrac{s\bar{u}}{a\cos\theta} + \alpha_R}{U_o/L} - \frac{\bar{v}/U_o}{a/L}\tan\theta\right)\frac{u'}{U_o} + \frac{U_o}{2\Omega L}\frac{L\eta'}{\cos\theta}\frac{\partial}{\partial\eta}\left(\frac{\bar{v}}{U_o}\cos\theta \ \frac{u'}{U_o}\right)$$

$$+ \frac{U_o}{2\Omega L}\frac{\lambda'}{\xi}\frac{\partial}{\partial\lambda}\left[\left(\frac{\xi\bar{w}}{U_o/L} - \frac{g\bar{M}_c}{p_o U_o/L}\right)\frac{u}{U_o}\right] - \frac{\lambda'}{\xi}\frac{\partial}{\partial\lambda}\ \xi\frac{\nu}{2\Omega H^2}\ \lambda'\frac{\partial(u'/U_o)}{\partial\lambda}$$

$$+ \; (\frac{U_o}{2\Omega L} \; Ln' \; \frac{\partial \bar{u}/U_o}{\partial \eta} - \frac{U_o}{2\Omega L} \; \frac{L}{a} \; \frac{\bar{u}}{U_o} \tan\theta - \frac{f}{2\Omega}) \; \frac{v'}{U_o} + \frac{U_o}{2\Omega L} \; (\lambda' \; \frac{\partial \bar{u}/U_o}{\partial \lambda}) \; \frac{w'}{U_o/L}$$

$$+ \; i \; \frac{s}{a\cos\theta} \; \frac{2\Omega U_o L}{2\Omega U_o} \; \frac{\Phi'}{2\Omega U_o L} + \frac{U_o}{2\Omega L} \; \frac{\lambda'}{\xi} \; \frac{\partial}{\partial \lambda} \; (\frac{g\bar{M}_c}{p_o U_o/L}) \; \frac{u'_c}{U_o}$$

$$= - \; \frac{U_o}{2\Omega L} \; \frac{\lambda'}{\xi} \; \frac{\partial}{\partial \lambda} \; [\frac{gM'_c}{p_o U_o/L} \; (\frac{\bar{u}_c}{U_o} - \frac{\bar{u}}{U_o})]$$

Rewriting this equation in an alternate form yields

$$R_o(-\frac{i\sigma}{U_o/L} + i\frac{s/s'}{\cos\theta} \; \bar{u}^* + \frac{\alpha_R}{U_o/L} - \frac{1}{s'} \; \bar{v}^* \tan\theta)u'^* + R_o \; \frac{Ln'}{\cos\theta} \; \frac{\partial}{\partial \eta}(\bar{v}^* \cos\theta u'^*)$$

$$+ \; R_o \; \frac{\lambda'}{\xi} \; \frac{\partial}{\partial \lambda} \; [(\xi \bar{w}^* - \bar{M}_c^*)u'^*] - \frac{\lambda'}{\xi} \; \frac{\partial}{\partial \lambda} \; \xi \; E_o \lambda' \; \frac{\partial u'^*}{\partial \lambda}$$

$$+ \; (R_o Ln' \; \frac{\partial \bar{u}^*}{\partial \eta} - R_o \; \frac{\bar{u}}{s'} \; \tan\theta - f^*)v'^* + R_o(\lambda' \; \frac{\partial \bar{u}^*}{\partial \lambda})w'^* \qquad (6.1)$$

$$+ \; \frac{is/s'}{\cos\theta} \; \Phi'^* + R_o \; \frac{\lambda'}{\xi} \; \frac{\partial}{\partial \lambda} \; (\bar{M}_c^*)u'_c^* = - R_o \; \frac{\lambda'}{\xi} \; \frac{\partial}{\partial \lambda} \; [M_c'^*(\bar{u}_c^* - \bar{u}^*)]$$

Similarly, by multiplying the v-momentum equation by $(1/2\Omega U_o)$, we can write

$$(\frac{U_o}{2\Omega L} \; \frac{L}{a} \; \frac{2\bar{u}}{U_o} \; \tan\theta + \frac{f}{2\Omega}) \; \frac{u'}{U_o} + \frac{U_o}{2\Omega L} \; (\frac{-i\sigma+i\frac{s\bar{u}}{a\cos\theta}+\alpha_R}{U_o/L} + Ln' \; \frac{\partial \bar{v}/U_o}{\partial \eta})\frac{v'}{U_o}$$

$$+ \; \frac{U_o}{2\Omega L} \; \frac{Ln'}{\cos\theta} \; \frac{\partial}{\partial \eta} \; (\frac{\bar{v}}{U_o} \; \cos\theta \; \frac{v'}{U_o}) + \frac{U_o}{2\Omega L} \; \frac{\lambda'}{\xi} \; \frac{\partial}{\partial \lambda} \; [(\xi \; \frac{\bar{w}}{U_o/L} - \frac{g\bar{M}_c}{p_o U_o/L})\frac{v'}{U_o}]$$

$$- \; \frac{\lambda'}{\xi} \; \frac{\partial}{\partial \lambda} \; \xi \; \frac{\nu}{2\Omega H^2} \; \lambda' \; \frac{\partial}{\partial \lambda} \; (\frac{v'}{U_o}) + \frac{U_o}{2\Omega L} \; (\lambda' \; \frac{\partial \bar{v}/U_o}{\partial \lambda}) \; \frac{w'}{U_o/L}$$

$$+ \; \frac{2\Omega U_o Ln'}{2\Omega U_o} \; \frac{\partial}{\partial \eta} \; \frac{\Phi'}{2\Omega U_o L} + \frac{U_o}{2\Omega L} \; \frac{\lambda'}{\xi} \; \frac{\partial}{\partial \lambda} \; (\frac{g\bar{M}_c}{p_o U_o/L}) \; \frac{v'_c}{U_o}$$

$$= - \frac{U_o}{2\Omega L} \frac{\lambda'}{\xi} \frac{\partial}{\partial \lambda} \left[\frac{gM'_c}{p_o U_o /L} \left(\frac{\bar{v}_c}{U_o} - \frac{\bar{v}}{U_o} \right) \right]$$

Alternately

$$(R_o \frac{2\bar{u}^*}{s'} \tan\theta + f^*)u'^* + R_o \left(\frac{-i\sigma}{U_o /L} + \frac{is/s'}{\cos\theta} \right) \bar{u}^* + \frac{\alpha_R}{U_o /L}$$

$$+ L\eta' \frac{\partial \bar{v}^*}{\partial \eta})v'^* + R_o \frac{L\eta'}{\cos\theta} \frac{\partial}{\partial \eta} (\bar{v}^* \cos\theta v'^*) + R_o \frac{\lambda'}{\xi} \frac{\partial}{\partial \lambda}$$

$$[(\xi \bar{w}^* - \bar{M}^*_c)v'^*] - \frac{\lambda'}{\xi} \frac{\partial}{\partial \lambda} \xi E_o \lambda' \frac{\partial v'^*}{\partial \lambda} + R_o (\lambda' \frac{\partial \bar{v}^*}{\partial \lambda})w'^*$$

$$+ L\eta' \frac{\partial \phi'^*}{\partial \eta} + R_o \frac{\lambda'}{\xi} \frac{\partial \bar{M}^*_c}{\partial \lambda} \quad v'^*_c = -R_o \frac{\lambda'}{\xi} \frac{\partial}{\partial \lambda} [M'^*_c (\bar{v}_c^* - \bar{v}^*)]$$

(6.2)

The hydrostatic approximation is multiplied by $(1/2\Omega LU_o)$ which yields

$$- \frac{RT'}{2\Omega LU_o} + \lambda' \frac{\partial}{\partial \lambda} \left(\frac{\phi'}{2\Omega LU_o} \right) = 0$$

Alternately,

$$-T'^* + \lambda' \frac{\partial \phi'^*}{\partial \lambda} = 0$$

(6.3)

The continuity equation is multiplied by (L/U_o)

$$\frac{is}{a\cos\theta} \frac{L}{U_o} u' + \frac{L}{U_o} \frac{\eta'}{\cos\theta} \frac{\partial}{\partial \eta} (v'\cos\theta) + \frac{\lambda'}{\xi} \frac{\partial}{\partial \lambda} (\xi w' \frac{L}{U_o}) = 0$$

Alternately

$$(\frac{is/s'}{\cos\theta}) u'^* + \frac{L\eta'}{\cos\theta} \frac{\partial}{\partial \eta} (v'^*\cos\theta) + \frac{\lambda'}{\xi} \frac{\partial}{\partial \lambda} (\xi w'^*) = 0$$

(6.4)

Finally the thermodynamic equation is multiplied by $(L/U_o \Gamma_1)$

$$\frac{L}{\Gamma_1} (\eta' \frac{\partial \bar{T}}{\partial \eta}) \frac{v'}{U_o} + \frac{L}{\Gamma_1} (\lambda' \frac{\partial \bar{T}}{\partial \lambda} + \kappa \bar{T}) \frac{w'}{U_o} + \frac{L}{U_o \Gamma_1} [-i\sigma + \frac{is\bar{u}}{a\cos\theta} + \alpha_N)T'$$

$$+ \bar{v}\eta' \frac{\partial T'}{\partial \eta} + e^{-\kappa z} \bar{w}\lambda' \frac{\partial}{\partial \lambda} (e^{\kappa z}T')] - \frac{L}{U_o\Gamma_1} \frac{\lambda'}{p/p_o} \frac{\partial}{\partial \lambda} \frac{p}{p_o} \frac{\hat{v}}{H^2} \lambda' \frac{\partial T'}{\partial \lambda}$$

$$= \frac{L}{U_o\Gamma_1} \frac{Q'}{c_p}$$

Alternately

$$[L\eta' \frac{\partial}{\partial \eta} (\frac{\bar{T}}{\Gamma_1})]v'^* + (\frac{\lambda' \frac{\partial \bar{T}}{\partial \lambda} + \kappa\bar{T}}{\Gamma_1})w'^* + R_o\varepsilon[(\frac{-i\sigma}{U_o/L} + \frac{is/s'}{\cos\theta} \bar{u}^* + \frac{\alpha_N}{U_o/L})$$

$$\text{(6.5)}$$

$$+ \bar{v}^*L\eta' \frac{\partial}{\partial \eta} + e^{-\kappa z} \bar{w}^* \lambda' \frac{\partial}{\partial \lambda} e^{\kappa z}]T'^* - \varepsilon \frac{\lambda'}{\xi} \frac{\partial}{\partial \lambda} \xi\hat{E}_o\lambda' \frac{\partial T'^*}{\partial \lambda} = Q'^*$$

7. Equations Written with Coefficients

As one can readily note from the previous section, the equations in their linearized non-dimensional flux form are rather lengthly and obviously would be cumbersome to work with. In view of this difficulty we have chosen to rewrite Eqs. 6.1-6.5 with coefficients which operate upon the non-dimensional dependent variables. With this strategy the appearance of the equations is simplified, and the programming aspects of the problem become more tractable. These coefficients are defined as follows:

$$A(\eta,\lambda) = R_o \left(\frac{-i\sigma}{U_o/L} + \frac{is/s'}{\cos\theta} \bar{u}^* \right) = \frac{U_o}{2\Omega L} \left(\frac{-i\sigma}{U_o/L} + \frac{is/s'}{\cos\theta} \frac{\bar{u}}{U_o} \right)$$

$$= \frac{-i\sigma}{2\Omega} + \frac{i(s/s')\bar{u}}{2\Omega L \cos\theta} = \frac{-i\sigma}{2\Omega} + i \frac{s}{\cos\theta} \frac{\bar{u}}{2\Omega a}$$

$$AR(\eta,\lambda) = A + R_o \frac{\alpha_R}{U_o/L} = A + \frac{U_o}{2\Omega L} \left(\frac{\alpha_R}{U_o/L} \right) = A + \frac{\alpha_R}{2\Omega}$$

$$AN(\eta,\lambda) = A + R_o \frac{\alpha_N}{U_o/L} = A + \frac{U_o}{2\Omega L} \left(\frac{\alpha_N}{U_o/L} \right) = A + \frac{\alpha_N}{2\Omega}$$

$$Q9(\eta,\lambda) = AR - R_o \frac{\bar{v}^*}{s'} \tan\theta = AR - \frac{U_o}{2\Omega L} \frac{\bar{v}}{s'U_o} \tan\theta = AR - \frac{\bar{v}}{2\Omega a} \tan\theta$$

$$P1(\eta) = R_o \frac{L\eta'}{\cos\theta} = \frac{U_o}{2\Omega L} \frac{L\eta'}{\cos\theta} = \frac{U_o}{2\Omega} \frac{\eta'}{\cos\theta}$$

$$P2(\eta,\lambda) = \bar{v}^* \cos\theta = \frac{\bar{v}}{U_o} \cos\theta$$

$$P3(\eta,\lambda) = R_o (\xi\bar{w}^* - \bar{M}_c^*) = \frac{U_o}{2\Omega L} \left(\frac{\xi\bar{w}}{U_o/L} - \frac{g\bar{M}_c}{p_o U_o/L} \right) = \frac{\xi\bar{w}}{2\Omega} - \frac{g\bar{M}_c}{2\Omega p_o}$$

$$D(\lambda) = \frac{\lambda'}{\xi}$$

$$E(\eta,\lambda) = \xi E_o \lambda'$$

$$F(\eta,\lambda) = \xi \hat{E}_o \lambda'$$

$$Q10(\eta,\lambda) = R_o L\eta' \frac{\partial \bar{u}^*}{\partial \eta} - R_o \frac{\bar{u}^*}{s'} \tan\theta - f^* = \frac{L\eta'}{2\Omega L} \frac{\partial \bar{u}}{\partial \eta} - \frac{\bar{u}}{2\eta a} \tan\theta - \frac{f}{2\Omega}$$

$$Q3(\eta,\lambda) = R_o \lambda' \frac{\partial \bar{u}^*}{\partial \lambda} = \frac{\lambda'}{2\Omega L} \frac{\partial \bar{u}}{\partial \lambda}$$

$$Q2(\eta) = i \frac{s/s'}{\cos\theta}$$

$$AL2(\eta,\lambda) = R_o \frac{\lambda'}{\xi} \frac{\partial}{\partial \lambda} \bar{M}_c^* = D \frac{\partial}{\partial \lambda} \frac{U_o}{2\Omega L} \frac{g\bar{M}_c}{p_o U_o/L} = D \frac{\partial}{\partial \lambda} \left(\frac{g\bar{M}_c}{2\Omega p_o}\right)$$

$$B1(\eta,\lambda) = -R_o \frac{\lambda'}{\xi} \frac{\partial}{\partial \lambda} [M_c'^*(\bar{u}_c^* - \bar{u}^*)] = D \frac{\partial}{\partial \lambda} \frac{U_o}{2\Omega L} \left[\frac{gM_c'}{p_o U_o/L} \left(\frac{\bar{u}}{U_o} - \frac{\bar{u}_c}{U_o}\right)\right]$$

$$= D \frac{\partial}{\partial \lambda} \left[\frac{gM_c'}{2\Omega p_o} \left(\frac{\bar{u}}{U_o} - \frac{\bar{u}_c}{U_o}\right)\right]$$

$$B2(\eta,\lambda) = -R_o \frac{\lambda'}{\xi} \frac{\partial}{\partial \lambda} [M_c'^* (\bar{v}_c^* - v^*)] = D \frac{\partial}{\partial \lambda} \frac{U_o}{2\Omega L} \left[\frac{gM_c'}{p_o U_c/L} \left(\frac{\bar{v}}{U_o} - \frac{\bar{v}_c}{U_o}\right)\right]$$

$$= D \frac{\partial}{\partial \lambda} \left[\frac{gM_c'}{2\Omega p_o} \left(\frac{\bar{v}}{U_o} - \frac{\bar{v}_c}{U_o}\right)\right]$$

$$B3(\eta,\lambda) = Q'^* = \frac{L}{U_o \Gamma_1} \frac{Q'}{c_p}$$

$$Q11(\eta,\lambda) = R_o \frac{2\bar{u}^*}{s'} \tan\theta + f^* = \frac{U_o}{2\Omega L} \frac{2\bar{u}}{s'U_o} \tan\theta + \frac{f}{2\Omega} = \frac{2\bar{u}\tan\theta}{2\Omega a} + \frac{f}{2\Omega}$$

$$Q13(\eta,\lambda) = AR + R_o L\eta' \frac{\partial \bar{v}^*}{\partial \eta} = AR + \frac{L\eta'}{2\Omega L} \frac{\partial \bar{v}}{\partial \eta}$$

$$Q5(\eta,\lambda) = R_o \lambda' \frac{\partial \bar{v}^*}{\partial \lambda} = \frac{\lambda'}{2\Omega L} \frac{\partial \bar{v}}{\partial \lambda}$$

$$C1(\eta) = L\eta' = \frac{a\eta'}{s'}$$

$$Q22(\eta) = \frac{is/s'}{\cos\theta}$$

$$C2(\eta) = \frac{L\eta'}{\cos\theta}$$

$$C3(\eta) = \cos\theta$$

$$C5(\lambda) = \xi$$

$$D2(\lambda) = \lambda'$$

$$Q6(\eta,\lambda) = \frac{L\eta'}{\Gamma_1} \frac{\partial \bar{T}}{\partial \eta}$$

$$Q7(\eta,\lambda) = \frac{1}{\Gamma_1} (\lambda' \frac{\partial \bar{T}}{\partial \lambda} + \kappa \bar{T})$$

$$C7(\lambda) = e^{\kappa z}$$

$$C8 = \varepsilon = \frac{4\Omega^2 L^2}{R\Gamma_1}$$

$$C8D(\lambda) = C8 \cdot D$$

$$CC = R_o \bar{v}^* L\eta' = \frac{U_o}{2\Omega L} \frac{\bar{v}}{U_o} L\eta' = \frac{\bar{v}}{2\Omega L} L\eta'$$

$$C6 = R_o e^{-\kappa z} \bar{w}^* \lambda' = \frac{U_o}{2\Omega L} e^{-\kappa z} \frac{\bar{w}L}{U_o} \lambda' = \frac{\bar{w}}{2\Omega} e^{-\kappa z} \lambda'$$

$$C8AN(\eta,\lambda) = C8 \cdot AN$$

$$C8CC(\eta,\lambda) = C8 \cdot CC$$

$$C8C6(\eta,\lambda) = C8 \cdot C6$$

By defining these coefficients, our systems of equations can now be written as:

u-Momentum (7.1)

$$\left(Q9 + P1 \frac{\partial}{\partial \eta} Pz + D \frac{\partial}{\partial \lambda} P3 - D \frac{\partial}{\partial \lambda} E \frac{\partial}{\partial \lambda}\right)u'^* + (Q10)w'^* + (Q3)w'^*$$

$$+ (Q2)\phi'^* + (AL2)U'^*_c = (B1)$$

v-Momentum (7.2)

$$(Q11)u'^* + \left(Q13 + P1 \frac{\partial}{\partial \eta} P2 + D \frac{\partial}{\partial \lambda} P3 - D \frac{\partial}{\partial \lambda} E \frac{\partial}{\partial \lambda}\right)v'^* + (Q5)w'^*$$

$$+ (C1) \frac{\partial \phi'^*}{\partial \eta} + (AL2)v'^*_c = (B2)$$

Continuity (7.3)

$$(Q22)u'^* + \left(C2 \frac{\partial}{\partial \eta} C3\right)v'^* + \left(D \frac{\partial}{\partial \lambda} C5\right)w'^* = 0$$

Thermodynamic (7.4)

$$(Q6)v'^* + (Q7)w'^* + \left(C8AN + C8CC \frac{\partial}{\partial \eta} + C8C6 \frac{\partial}{\partial \lambda} C7 - C8D \frac{\partial}{\partial \lambda} F \frac{\partial}{\partial \lambda}\right)T'^* = (B3)$$

Hydrostatic Approximation (7.5)

$$-T'^* + (D2) \frac{\partial \phi'^*}{\partial \lambda} = 0$$

8. Discretized Equation

The equations 7.1-7.5 are finite differenced in the latitudinal and vertical directions. To do this we define the following:

$$\eta_i = \eta_s + (i - 1) \Delta\eta \text{ where } i \to 1, \text{ IY}$$

$$\lambda_j = \lambda_1 + (j - 1) \Delta\lambda \text{ where } j \to 1, \text{ IZ}$$

where $\eta_s \equiv \eta$ at southern boundary of model

IY $\equiv$ number of nodes in the latitudinal direction

$\lambda_1 \equiv \lambda$ at top of model atmosphere

IZ $\equiv$ number of level in the vertical direction

For brevity we drop the ()* notation, but it must be realized that dependent variables are still non-dimensional. The discretized equations are shown below:

u-Momentum   (8.1)

$$Q9_{ij}\, u'_{ij} \;+\; P1_{ij} \left[\frac{(P2u')_{i+1,j} - (P2u')_{i-1,j}}{2\Delta\eta} \right] \;+\; D_{ij} \left[\frac{(P3u')_{i,j+1} - (P3u')_{i,j-1}}{2\Delta\lambda} \right]$$

$$-\,D_{ij}\,\frac{1}{\Delta\lambda} \left[E_{i,j+\frac{1}{2}}\, \frac{u'_{i,j+1} - u'_{i,j}}{\Delta\lambda} \;-\; E_{i,j-\frac{1}{2}}\, \frac{u'_{i,j} - u'_{i,j-1}}{\Delta\lambda} \right] \;+\; Q10_{ij}\, v'_{ij} \;+\; Q3_{ij}\, w'_{ij}$$

$$+\,Q2_{ij}\, \Phi'_{ij} \;+\; AL2_{ij}\, u'_{ci} \;=\; B1_{ij}$$

26

v-Momentum (8.2)

$$Q11_{ij}\, u'_{ij} \;+\; Q13\, v'_{ij} \;+\; P1_{ij}\left[\frac{(P2\,v')_{i+1,j} - (P2\,v')_{i-1,j}}{2\Delta\eta}\right]$$

$$+\, D_{ij}\left[\frac{(P3\,v')_{i,j+1} - (P3\,v')_{i,j-1}}{2\Delta\lambda}\right] \;-\; D_{ij}\,\frac{1}{\Delta\lambda}\left[E_{i,j+\frac{1}{2}}\frac{v'_{i,j+1}-v'_{ij}}{\Delta\lambda} - E_{i,j-\frac{1}{2}}\frac{v'_{ij}-v'_{i,j-1}}{\Delta\lambda}\right]$$

$$+\, Q5_{ij}\, w'_{ij} \;+\; C1\left[\frac{\Phi'_{i+1,j} - \Phi'_{i-1,j}}{2\Delta\eta}\right] \;+\; AL2_{ij}\, v'_{ci} \;=\; B2_{ij}$$

Continuity (8.3)

$$Q22_{ij}\, u'_{ij} \;+\; C2_{ij}\left[\frac{(C3\,v')_{i+1,j} - (C3\,v')_{i-1,j}}{2\Delta\eta}\right]$$

$$+\, D_{ij}\left[\frac{(C5\,w')_{i,j+1} - (C5\,w')_{i,j-1}}{2\Delta\lambda}\right] \;=\; 0$$

Thermodynamic (8.4)

$$Q6_{ij}\, v'_{ij} \;+\; Q7_{ij}\, w'_{ij} \;+\; C8AN_{ij}\, T'_{ij}$$

$$+\, C8CC_{ij}\left[\frac{T'_{i+1,j} - T'_{i-1,j}}{2\Delta\eta}\right] \;+\; C8C6_{ij}\left[\frac{(C7\cdot T')_{i,j+1} - (C7\cdot T')_{i,j-1}}{2\Delta\lambda}\right]$$

$$-\, C8D_{ij}\,\frac{1}{\Delta\lambda}\left[F_{i,j+\frac{1}{2}}\frac{T'_{i,j+1}-T'_{ij}}{\Delta\lambda} - F_{i,j-\frac{1}{2}}\frac{T'_{ij}-T'_{i,j-1}}{\Delta\lambda}\right] \;=\; B3_{ij}$$

Hydrostatic Approximation (8.5)

$$-\, T'_{ij} \;+\; D2_{ij}\left[\frac{\Phi'_{i,j+1} - \Phi'_{i,j-1}}{2\Delta\lambda}\right] \;=\; 0$$

9. Matrix Form of Equation

To aid us in solving the system of equations given in 8.1-8.5, it is convenient to conceptualize these equations at each point in the model's domain in the form of Eq. 9.1.

$$(9.1)$$

$$LL_{ij}X_{i,j-1} + AK_{ij}X_{i-1,j} + BK_{ij}X_{ij} + CK_{ij}X_{i+1,j} + UU_{ij}X_{i,j+1} + J_{ij}X_{ci} = B_{ij}$$

where $X_{ij} = \begin{pmatrix} u' \\ v' \\ w' \\ T' \\ \Phi' \end{pmatrix}_{ij}$ represents all perturbation variables at the (i,j) grid point

and LL_{ij}, UU_{ij}, J_{ij}, B_{ij}, AK_{ij}, BK_{ij} and CK_{ij} are defined as follows:

$$LL_{ij} = \begin{bmatrix} D_j\left(\dfrac{-P3_{i,j-1}}{2\Delta\lambda} - \dfrac{E_{i,j-\frac{1}{2}}}{\Delta\lambda^2}\right) & 0 & 0 & 0 & 0 \\ 0 & D_j\left(\dfrac{-P3_{ij-1}}{2\Delta\lambda} - \dfrac{E_{ij-\frac{1}{2}}}{\Delta\lambda^2}\right) & 0 & 0 & 0 \\ 0 & 0 & -D_j\left(\dfrac{C5_{j-1}}{2\Delta\lambda}\right) & 0 & 0 \\ 0 & 0 & 0 & \left[C8C6_{ij}\left(\dfrac{C7_{j-1}}{2\Delta\lambda}\right) - \dfrac{C8D_j}{\Delta\lambda^2}F_{ij-\frac{1}{2}}\right] & 0 \\ 0 & 0 & 0 & 0 & \dfrac{-D2_j}{2\Delta\lambda} \end{bmatrix}$$

$$UU_{ij} = \begin{bmatrix} D_j\left(\dfrac{P3_{i,j+1}}{2\Delta\lambda} - \dfrac{E_{i,j+\frac{1}{2}}}{\Delta\lambda^2}\right) & 0 & 0 & 0 & 0 \\ 0 & D_j\left(\dfrac{P3_{ij+1}}{2\Delta\lambda} - \dfrac{E_{ij+\frac{1}{2}}}{\Delta\lambda^2}\right) & 0 & 0 & 0 \\ 0 & 0 & D_j\left(\dfrac{C5_{j+1}}{2\Delta\lambda}\right) & 0 & 0 \\ 0 & 0 & 0 & \left[C8C6_{ij}\left(\dfrac{C7_{j+1}}{2\Delta\lambda}\right) - \dfrac{C8D}{\Delta\lambda^2}F_{ij+\frac{1}{2}}\right] & 0 \\ 0 & 0 & 0 & 0 & \dfrac{D2_j}{2\Delta\lambda} \end{bmatrix}$$

$$
J_{ij} = \begin{bmatrix}
AL2_{ij} & 0 & 0 & 0 & 0 \\
0 & AL2_{ij} & 0 & 0 & 0 \\
0 & 0 & 0 & 0 & 0 \\
0 & 0 & 0 & 0 & 0 \\
0 & 0 & 0 & 0 & 0
\end{bmatrix}
$$

$$
B_{ij} = \begin{bmatrix}
B1_{ij} \\
B2_{ij} \\
0 \\
B3_{ij} \\
0
\end{bmatrix}
$$

$$
AK_{ij} = \begin{bmatrix}
P1_i\left(\frac{-P2_{i-1,j}}{2\Delta\eta}\right) & 0 & 0 & 0 & 0 \\
0 & P1_i\left(\frac{-P2_{i-1,j}}{2\Delta\eta}\right) & 0 & 0 & \frac{-C1_i}{2\Delta\eta} \\
0 & \frac{-C2_i\,C3_{i-1}}{2\Delta\eta} & 0 & 0 & 0 \\
0 & 0 & 0 & \frac{-C8CC_{ij}}{2\Delta\eta} & 0 \\
0 & 0 & 0 & 0 & 0
\end{bmatrix}
$$

$$
BK_{ij} = \begin{bmatrix}
Q9_{ij}+\frac{D_j}{\Delta\chi^2}\left(E_{ij+\frac{1}{2}}+E_{ij-\frac{1}{2}}\right) & Q10_{ij} & Q3_{ij} & 0 & Q2_i \\
Q11_{ij} & Q13_{ij}+\frac{D_j}{\Delta\chi}\left(E_{i,j+\frac{1}{2}}+E_{i,j-\frac{1}{2}}\right) & Q5_{ij} & 0 & 0 \\
Q22_{ij} & 0 & 0 & 0 & 0 \\
0 & Q6_{ij} & Q7_{ij} & \left[CBAN_{ij}+\frac{C8D_j}{\Delta\chi^2}\left(E_{i,j+\frac{1}{2}}+E_{i,j-\frac{1}{2}}\right)\right] & 0 \\
0 & 0 & 0 & -1 & 0
\end{bmatrix}
$$

$$
CK_{ij} = \begin{bmatrix}
P1_i\left(\frac{P2_{i+1,j}}{2\Delta\eta}\right) & 0 & 0 & 0 & 0 \\
0 & P1_i\left(\frac{P2_{i+1,j}}{2\Delta\eta}\right) & 0 & 0 & \frac{C1_i}{2\Delta\eta} \\
0 & \frac{C2_i\,C3_{i+1}}{2\Delta\eta} & 0 & 0 & 0 \\
0 & 0 & 0 & \frac{C8CC_{ij}}{2\Delta\eta} & 0 \\
0 & 0 & 0 & 0 & 0
\end{bmatrix}
$$

10. Boundary Conditions

Since our system of equations can be reduced to an eighth order differential equation in the vertical, the continuous solution requires eight boundary conditions at the top and bottom of the model. These boundary conditions are given as follows:

at the upper boundary:

$$\frac{\partial u}{\partial \lambda} = \frac{\partial v}{\partial \lambda} = \frac{\partial T}{\partial \lambda} = 0 \quad \text{(due to large dissipation)}$$

$w = 0$ (rigid upper lid)

at the lower boundary:

$w = 0$ (an approximation to vertical z-velocity vanishing)

$$\frac{\partial u}{\partial \lambda} = BC1 \cdot u$$

$$\frac{\partial v}{\partial \lambda} = BC2 \cdot v \qquad \text{bulk aerodynamic parameterization}$$

$$\frac{\partial T}{\partial \lambda} = BC3 \cdot T$$

where

$$
\begin{matrix}
BC1 \\
BC2 \\
BC3
\end{matrix}
= \frac{\bar{H}_o \cdot CD \cdot V_o}{\lambda'}
\quad
\begin{matrix}
\nu_o^{-1} \\
\nu_o^{-1} \\
\hat{\nu}_o^{-1}
\end{matrix}
$$

$$\bar{H}_o = \frac{R\tilde{T}_o}{g}$$

$$\nu_o = \nu(z = 0)$$

$$\hat{\nu}_o = \hat{\nu}(z = 0)$$

The constants T_o, CD, V_o are defined in section 2.

To evaluate the λ-derivatives on the top and bottom boundaries we use a lower accuracy one-sided derivative. With the boundary conditions discussed above the matrix form of the equations at the top and bottom levels of the models are as follows.

Top: $j = 1$: $LL = AK = CK = JJ = B = 0$: $BK_{ij} + UU_{ij}\psi_{i,j+1} = 0$

where BK_{ij} and UU_{ij} are as follows:

$$BK_{ij} = \begin{bmatrix} -1 & 0 & 0 & 0 & 0 \\ 0 & -1 & 0 & 0 & 0 \\ 0 & 0 & 1 & 0 & 0 \\ 0 & 0 & 0 & -1 & 0 \\ 0 & 0 & 0 & -1 & \frac{-D2_j}{\Delta\lambda} \end{bmatrix} \qquad UU_{ij} = \begin{bmatrix} 1 & 0 & 0 & 0 & 0 \\ 0 & 1 & 0 & 0 & 0 \\ 0 & 0 & 0 & 0 & 0 \\ 0 & 0 & 0 & 1 & 0 \\ 0 & 0 & 0 & 0 & \frac{D2_j}{\Delta\lambda} \end{bmatrix}$$

Bottom: $j = IZ$: $UU = AK = CL = JJ = B = 0$: $LL_{ij}\psi_{i,j-1} + BK_{ij}\psi_{ij} = 0$

where BK_{ij} and LL_{ij} are as follows:

$$BK_{ij} = \begin{bmatrix} (1-\Delta\lambda\cdot BCU) & 0 & 0 & 0 & 0 \\ 0 & (1-\Delta\lambda\cdot BCV) & 0 & 0 & 0 \\ 0 & 0 & 1 & 0 & 0 \\ 0 & 0 & 0 & (1-\Delta\lambda\cdot BCT) & 0 \\ 0 & 0 & 0 & -1 & \frac{D2_j}{\Delta\lambda} \end{bmatrix} \qquad LL_{ij} = \begin{bmatrix} -1 & 0 & 0 & 0 & 0 \\ 0 & -1 & 0 & 0 & 0 \\ 0 & 0 & 0 & 0 & 0 \\ 0 & 0 & 0 & -1 & 0 \\ 0 & 0 & 0 & 0 & \frac{-D2_j}{\Delta\lambda} \end{bmatrix}$$

In the horizontal direction the system of equations is second order, so that two boundary conditions are required on the sides of the model. These boundary conditions were chosen as $v=0$ which inhibits flow through the side boundaries of the model. By setting $\bar{v}=0$ at $i=1$ and $i=IY$, the following coefficients: P2, Q5, B2, CC, and C8CC are zero on the side boundaries with one-sided finite differences. By replacing the v-momentum equation on the side with $v=0$, the matrix form of the equations on the sides is altered as shown below.

AT i = 1:

$$LL_{ij} = UU_{ij} = J_{ij} = B_{ij} = AK_{ij} = BK_{ij} = CK_{ij} = 0 \quad \text{for row 2}$$

$$BK_{ij}(2,2) = 1$$

$$AK_{ij} = 0$$

$CK_{ij}=2.\times$ old CK_{ij} [including changes above] so that each denominator is $\Delta\eta$, not $2\Delta\eta$

$$BK_{ij} = \text{old } BK_{ij} + \begin{bmatrix} 0 & 0 & 0 & 0 & 0 \\ 0 & 0 & 0 & 0 & 0 \\ 0 & \dfrac{-C2(1)\cdot C3(1)}{\Delta\eta} & 0 & 0 & 0 \\ 0 & 0 & 0 & 0 & 0 \\ 0 & 0 & 0 & 0 & 0 \end{bmatrix}$$

AT i = IY

$$LL_{IY,j}=UU_{IY,j}=J_{IY,j}=B_{IY,j}=AK_{IY,j}=BK_{IY,j}=CK_{IY,j}=0 \quad \text{for row 2 in metrices}$$

$$BK_{IY,j}(2,2) = 1$$

$AK_{IY,j} = 2.\times$ old $AK_{IY,j}$ [including changes above] so that each denominator is $\Delta\eta$, not $2\Delta\eta$

$$CK_{IY,j} = 0$$

$$BK_{IY,j} = \text{old } BK_{IY,j} + \begin{bmatrix} 0 & 0 & 0 & 0 & 0 \\ 0 & \dfrac{C2(IY)\cdot C3(IY)}{\Delta\eta} & 0 & 0 & 0 \\ 0 & 0 & 0 & 0 & 0 \\ 0 & 0 & 0 & 0 & 0 \\ 0 & 0 & 0 & 0 & 0 \end{bmatrix}$$

11. Algorithm for Solving Problem

For a specific heating function (Q'), the response in the perturbation fields of the three-dimensional wind (u',v',w'), geopotential (Φ'), and temperature (T') are calculated from Eqs. 8.1-8.5. The algorithm which solves for these perturbation fields can be divided into the following three sections.

11.1) Filling of matrices

11.2) Gaussian elimination

11.3) Backsubstitution

Each of these sections will be discussed in the order that they appear in our computer algorithm which is flowcharted in the Appendix.

11.1 Filling of matrices

By combining Eq. 9.1 for all the horizontal nodes on a level, we can write an equation for each level in the model as follows:

$$L_j X_{j-1} + D_j X_j + U_j X_{j+1} + J_j X_c = B_j \tag{11.1}$$

where $j \equiv$ vertical level of model. The X_j is a column vector which consists of the IY grid point vectors $x_{ij} \equiv (u'_{ij}, v'_{ij}, w'_{ij}, T'_{ij}, \Phi'_{ij})^T$ in sequence. B_j is a similar column vector

$$X_j \equiv \begin{pmatrix} (x_{1j}) \\ (x_{2j}) \\ (x_{3j}) \\ \vdots \\ (x_{IY,j}) \end{pmatrix} \qquad B_j \equiv \begin{pmatrix} (B_{1j}) \\ (B_{2j}) \\ (B_{3j}) \\ \vdots \\ (B_{IY,j}) \end{pmatrix}$$

The L_j, U_j, and J_j matrices are block diagonal, with the $i\underline{\text{th}}$ block sub-matrix being LL_{ij}, UU_{ij}, JJ_{ij}, repectively. From Section 9,

LL_{ij}, UU_{ij}, and JJ_{ij} are themselves diagonal 5 by 5 sub-matrices. For example,

$$L_j \equiv \begin{pmatrix} (LL_{ij}) & & & \\ & (LL_{2j}) & & \\ & & \ddots & \\ & & & (LL_{IY,j}) \end{pmatrix}$$

U_j and J_j are similarly diagonal matrices. L_j, U_j and J_j each involve storage of 5 × IY elements on the diagonal. The D_j matrix, which is a combination of the $AK_{i,j}$, $BK_{i,j}$, and $CK_{i,j}$ operators from Eq. 9.1, is a block tri-diagonal matrix, with each block a 5 by 5 submatrix. At some vertical level j:

$$D_j = \begin{bmatrix} BK_{1,j} & CK_{1,j} & & & & & & & & \\ AK_{2,j} & BK_{2,j} & CK_{2,j} & & & & & 0's & & \\ & AK_{3,j} & BK_{3,j} & CK_{3,j} & & & & & & \\ & & AK_{4,j} & BK_{4,j} & CK_{4,j} & & & & & \\ & & & \ddots & \ddots & \ddots & & & & \\ & & & & AK_{IY-3,j} & BK_{IY-3,j} & CK_{IY-3,j} & & & \\ & & & & & AK_{IY-2,j} & BK_{IY-2,j} & CK_{IY-2,j} & & \\ & 0's & & & & & AK_{IY-1,j} & BK_{IY-1,j} & CK_{IY-1,j} \\ & & & & & & & AK_{IY,j} & BK_{IY,j} \end{bmatrix}$$

Since D_j is a block tri-diagonal matrix, in storing D_j we have taken advantage of the fact that most of its elements are zero. In storage the compressed matrix D at any vertical level appears as follows:

$$D_j = \begin{bmatrix} BK_{1,j} & CK_{1,j} & CK_{2,j} & \cdots & CK_{i-1,j} & \cdots & CK_{IY-3,j} & CK_{IY-2,j} & 0 \\ AK_{2,j} & BK_{2,j} & BK_{3,j} & \cdots & BK_{i,j} & \cdots & BK_{IY-2,j} & BK_{IY-1,j} & CK_{IY-1,j} \\ 0 & AK_{3,j} & AK_{4,j} & \cdots & AK_{i+1,j} & \cdots & AK_{IY-1,j} & AK_{IY,j} & BK_{IY,j} \end{bmatrix}$$

When D is needed for computation, it is reformed into its original sparse structure. The memory requirements for storing the compressed version of D over its sparse structure are reduced by a factor of (IY/3). For example with typical values needed to resolve wave structure of IY = 21 and IZ = 31, the storage of the full matrix D for all levels in the models would require $\sim 10^6$ words of memory. On the other hand, the compressed D matrixes would require only $\sim 1.3 \times 10^5$ words of memory or a factor of 8 less! By storing the matrices in Eq. 11.1 as outlined above, the CRAY computer can easily contain in its memory these matrices for all the levels in the model simultaneously.

Filling the matrices in Eq. 11.1 at a specific vertical level, requires that the component sub-matrices: UU, LL, JJ, BV, AK, BK, and CK be filled first at each horizontal node on that level. Once these sub-matrices are defined they are used to form the L, U, J, B, and D matrices at one vertical level. By repeating this process at each level in the model, our system of equations can now be represented in the form of the linear matrix equation, AX = B* which is shown schematically below.

$$
\begin{bmatrix}
D_1 & U_1 & & & & & J_1 & & \\
L_2 & D_2 & U_2 & & & & J_2 & & \\
& L_3 & D_3 & U_3 & & & J_3 & & \\
& & & & L_{\ell-1} & D_{\ell-1} & (U+J)_{\ell-1} & & \\
& & & & & L_\ell & (D+J)_\ell & U_\ell & \\
& & & & & & (L+J)_{\ell+1} & D_{\ell+1} & U_{\ell+1} \\
& & & & & & & L_{IZ} & D_{IZ}
\end{bmatrix}
\begin{bmatrix}
X_1 \\ X_2 \\ X_3 \\ X_{\ell-1} \\ X_\ell \\ X_{\ell+1} \\ X_{IZ}
\end{bmatrix}
=
\begin{bmatrix}
B_1 \\ B_2 \\ B_3 \\ B_{\ell-1} \\ B_\ell \\ B_{\ell+1} \\ B_{IZ}
\end{bmatrix}
$$

We have assumed here that $J_j=0$ (i.e. no cloud mass flux) for $j>\ell+1$. The parameter 'ℓ' as it appears here is defined as the level of cloud base and is computed from Eq. 11.2

$$\ell = \text{IFIX}(\lambda(ZC)/\text{DLAM} + 0.5) \qquad (11.2)$$

where $\text{DLAM} = (\lambda_{IZ} - \lambda_1)/(IZ - 1)$

Because the vertical differentiation is at most second-order in the five variables, only vertical grid levels separated by $\Delta\lambda$ and $2\Delta\lambda$ are related in the finite difference scheme. Thus the matrix A is a block tridiagonal matrix, with blocks of dimension 5×IY by 5×IY.

11.2 Gaussian elimination scheme

To reduce the linear matrix system $AX = B^*$ to an upper triangular matrix, we employ a Gaussian elimination scheme, slightly modified for the cumulus friction terms, from a version suggested by Lindzen and Kou (1969). In this scheme, IZ matrices (5×IY by 5×IY) must be inverted in full-storage (non-sparse) mode. The procedure for using this scheme at the various levels in the model is shown below.

$$j=1$$

$$D_1 X_1 + U_1 X_2 + J_1 X_\ell = B_1$$
$$X_1 + D_1^{-1} U_1 X_2 + D_1^{-1} J_1 X_\ell = D_1^{-1} B_1$$
$$X_1 + \alpha_1 X_2 + \beta_1 X_\ell = \gamma_1$$

$$\delta_1 = D_1^{-1}$$
$$\alpha_1 = \delta_1 U_1$$
$$\beta_1 = \delta_1 J_1$$
$$\gamma_1 = \delta_1 B_1$$

$$j = 2, 3, \ldots, \ell-2$$

$$(-L_j) \cdot \{ X_{j-1} + \alpha_{j-1} X_j + \beta_{j-1} X_\ell = \gamma_{j-1} \}$$
$$\underline{L_j X_{j-1} + D_j X_j + U_j X_{j+1} + J_j X_\ell = B_j}$$
$$(D_j - L_j \alpha_{j-1}) X_j + (U_j) X_{j+1} + (J_j - L_j \beta_{j-1}) X_\ell = (B_j - L_j \gamma_{j-1})$$
$$X_j + (\delta_j U_j) X_{j+1} + \delta_j (J_j - L_j \beta_{j-1}) X_\ell = \delta_j (B_j - L_j \gamma_{j-1})$$
$$X_j + \alpha_j X_{j+1} + \beta_j X_\ell = \gamma_j$$

$$\delta_j = (D_j - L_j \alpha_{j-1})^{-1}$$
$$\alpha_j = \delta_j U_j$$
$$\beta_j = \delta_j (J_j - L_j \beta_{j-1})$$
$$\gamma_j = \delta_j (B_j - L_j \gamma_{j-1})$$

$$j = \ell-1$$

$$(-L_{\ell-1}) \cdot \{ X_{\ell-2} + \alpha_{\ell-2} X_{\ell-1} + \beta_{\ell-2} X_\ell = \gamma_{\ell-2} \}$$

$$L_{\ell-1} X_{\ell-2} + D_{\ell-1} X_{\ell-1} + (U+J)_{\ell-1} X_\ell = B_{\ell-1}$$

$$(D_{\ell-1} - L_{\ell-1} \alpha_{\ell-2}) X_{\ell-1} + ((U+J)_{\ell-1} - L_{\ell-1} \beta_{\ell-2}) X_\ell = (B_{\ell-1} - L_{\ell-1} \gamma_{\ell-2})$$

$$X_{\ell-1} + \alpha_{\ell-1} X_\ell = \gamma_{\ell-1}$$

$$\delta_{\ell-1} = (D_{\ell-1} - L_{\ell-1} \alpha_{\ell-2})^{-1}$$
$$\alpha_{\ell-1} = \delta_{\ell-1} [(U+J)_{\ell-1} - L_{\ell-1} \beta_{\ell-2}]$$
$$\gamma_{\ell-1} = \delta_{\ell-1} (B_{\ell-1} - L_{\ell-1} \gamma_{\ell-2})$$

$$j = \ell$$

$$(-L_\ell) \cdot \{ X_{\ell-1} + \alpha_{\ell-1} X_\ell = \gamma_{\ell-1} \}$$

$$L_\ell X_{\ell-1} + (D+J)_\ell X_\ell + U_\ell X_{\ell+1} = B_\ell$$

$$((D+J)_\ell - L_\ell \alpha_{\ell-1}) X_\ell + U_\ell X_{\ell+1} = B_\ell - L_\ell \gamma_{\ell-1}$$

$$X_\ell + \alpha_\ell X_{\ell+1} = \gamma_\ell$$

$$\delta_\ell = [(D+J)_\ell - L_\ell \alpha_{\ell-1}]^{-1}$$
$$\alpha_\ell = \delta_\ell U_\ell$$
$$\gamma_\ell = \delta_\ell (B_\ell - L_\ell \gamma_{\ell-1})$$

$$j = \ell+1$$

If $\ell+1 < IZ$:

$$-(L+J)_{\ell+1} \{ X_\ell + \alpha_\ell X_{\ell+1} = \gamma_\ell \}$$

$$(L+J)_{\ell+1} X_\ell + D_{\ell+1} X_{\ell+1} + U_{\ell+1} X_{\ell+2} = B_{\ell+1}$$

$$[D_{\ell+1} - (L+J)_{\ell+1} \alpha_\ell] X_{\ell+1} + U_{\ell+1} X_{\ell+2} = B_{\ell+1} - (L+J)_{\ell+1} \gamma_\ell$$

$$X_{\ell+1} + \alpha_{\ell+1} X_{\ell+2} = \gamma_{\ell+1}$$

$$\delta_{\ell+1} = [D_{\ell+1} - (L+J)_{\ell+1} \alpha_\ell]^{-1}$$
$$\alpha_{\ell+1} = \delta_{\ell+1} U_{\ell+1}$$
$$\gamma_{\ell+1} = \delta_{\ell+1} [B_{\ell+1} - (L+J)_{\ell+1} \gamma_\ell]$$

If $\ell+1 = IZ$:

$$-(L+J)_{\ell+1} \cdot \{ X_\ell + \alpha_\ell X_{\ell+1} = \gamma_\ell \}$$

$$(L+J)_{\ell+1} X_\ell + D_{\ell+1} X_{\ell+1} = B_{\ell+1}$$

$$[D_{\ell+1} - (L+J)_{\ell+1} \alpha_\ell] X_{\ell+1} = B_{\ell+1} - (L+J)_{\ell+1} \gamma_\ell$$

$$X_{\ell+1} = \gamma_{\ell+1}$$

$$\delta_{\ell+1} = [D_{\ell+1} - (L+J)_{\ell+1} \alpha_\ell]^{-1}$$
$$\gamma_{\ell+1} = \delta_{\ell+1} [B_{\ell+1} - (L+J)_{\ell+1} \gamma_\ell]$$

$$j = \ell+2, \ell+3, \ldots IZ-1$$

If $\underline{\ell+1 < IZ}$:

$$(-L_j)\cdot\{ x_{j-1} + \alpha_{j-1} x_j = \gamma_{j-1}\}$$
$$\underline{L_j x_{j-1} + D_j x_j + U_j x_{j+1} = B_j}$$
$$(D_j - L_j \alpha_{j-1}) x_j + U_j x_{j+1} = B_j - L_j \gamma_{j-1}$$
$$x_j + \alpha_j x_{j+1} = \gamma_j$$

$$\delta_j = (D_j - L_j \alpha_{j-1})^{-1}$$
$$\alpha_j = \delta_j U_j$$
$$\gamma_j = \delta_j (B_j - L_j \gamma_{j-1})$$

$$j = IZ$$

If $\underline{\ell+1 < IZ}$:

$$(-L_{IZ})\cdot\{ x_{IZ-1} + \alpha_{IZ-1} x_{IZ} = \gamma_{IZ-1}\}$$
$$\underline{L_{IZ} x_{IZ-1} + D_{IZ} x_{IZ} = B_{IZ}}$$
$$(D_{IZ} - L_{IZ} \alpha_{IZ-1}) x_{IZ} = (B_{IZ} - L_{IZ} \gamma_{IZ-1})$$
$$x_{IZ} = \gamma_{IZ}$$

$$\delta_j = (D_j - L_j \alpha_{j-1})^{-1}$$
$$\gamma_j = \delta_j (B_j - L_j \gamma_{j-1})$$

The following table summarizes the form of the operators that are used in the Gaussian elimination scheme at the various levels (j) of the model.

j	δ_j	α_j	β_j	γ_j
1	D_j^{-1}	$\delta_j U_j$	$\delta_j J_j$	$\delta_j B_j$
$[2, \ell-2]$	$(D_j - L_j \alpha_{j-1})^{-1}$	$\delta_j U_j$	$\delta_j(J_j - L_j \beta_{j-1})$	$\delta_j(B_j - L_j \gamma_{j-1})$
$\ell-1$	$(D_j - L_j \alpha_{j-1})^{-1}$	$\delta_j[(U+J)_j - L_j \beta_{j-1}]$	——	$\delta_j(B_j - L_j \gamma_{j-1})$
ℓ	$[(D+J)_j - L_j \alpha_{j-1}]^{-1}$	$\delta_j U_j$	——	$\delta_j(B_j - L_j \gamma_{j-1})$
$[\ell+1, IZ-1]$	$[D_j - (L_j + \Delta_{j,\ell+1} J_{\ell+1})\alpha_{j-1}]^{-1}$	$\delta_j U_j$	——	$\delta_j[B_j - (L_j + \Delta_{j,\ell+1} J_{\ell+1})\gamma_{j-1}]$
IZ	$[D_j - (L_j + \Delta_{j,\ell+1} J_{\ell+1})\alpha_{j-1}]^{-1}$	——	——	$\delta_j[B_j - (L_j + \Delta_{j,\ell+1} J_{\ell+1})\gamma_{j-1}]$

where $\Delta_{j,\ell+1} = \begin{cases} 0 & \text{if } j \neq \ell+1 \\ 1 & \text{if } j = \ell+1 \end{cases}$

In an elegant extension of the Lindzen-Kuo method, Professor Paul Duchateau of the Mathematics Department of CSU developed a scheme to solve the linear matrix equation $AX = B*$ with a considerable reduction in computer time. He observed that each of the five equations involves a vertical derivative in a single variable, and this variable is different for each equation: specifically, u', v', w', T', Φ' in that order. These equations are not all second order in the vertical, so we cannot directly use use the Lindzen-Kuo scheme. However, if we finite difference them as they appear, without combining them, and retain all five variables as unknowns, we find again a block tridiagonal structure; but the off-diagonal blocks are themselves diagonal matrices! This is precisely the matrix structure outlined above.

Duchateau noted that with non-vanishing viscosity and thermal diffusivity, the off-diagnonal block matrices are guaranteed to be trivially invertable. Consequently, the algorithm can be modified so that only a single $5 \times IY$ by $5 \times IY$ dense matrix need be inverted. In the standard method, such a matrix inversion must be accomplished at each vertical level. Thus Duchateaus's scheme reduces the matrix inversion workload, which constitutes the primary computational burden, by a factor of IZ which is typically a factor of 30 or more.

In testing this scheme, we determined that its usefulness is limited to cases where viscosity is rather large (e.g. 100 m^2s^{-1}) throughout the model's domain. The restriction of this scheme results from using the L^{-1} matrix, which is inversely related to viscosity and diffusivity , to operate on a row of matrix A in reducing it to an upper triangular system (refer to schematic of $AX = B*$ of Section 11.1). Apparently when the magnitude of L is small (due to a small value of

viscosity; e.g. $\nu \leq 50$ m²s^{-1}), the condition number of the matrix to be inverted increases so that for all practical purposes the matrix is uninvertible.

Heuristically, all the ill-behaved aspects with small dissipation are collected into a single matrix inversion stage, which the algorithm cannot properly handle. When the ill behavior is distributed over many (time-consuming) matrix inversions, the algorithm works quite adequately. This result is apparently an application of the computer proverb, "You don't get something for nothing". Note, however, that Duchateau's scheme may be useful in second-order, dissipation-dominated problems. Unfortunately, that is not our area of interest.

11.3 Backsubstitution

Once the system AX = B* has been reduced to upper triangular form as shown below, it becomes a trival matter to solve for the solution matrix X.

$$
\begin{bmatrix}
I & \alpha_1 & & & & \beta_1 & & & \\
& I & \alpha_2 & & & \beta_2 & & & \\
& & I & \alpha_3 & & \beta_3 & & & \\
& & & & I & \alpha_{\ell-1} & & & \\
& & & & & I & \alpha_\ell & & \\
& & & & & & I & \alpha_{\ell+1} & \\
& & & & & & & & I
\end{bmatrix}
\begin{bmatrix}
X_1 \\ X_2 \\ X_3 \\ X_{\ell-1} \\ X_\ell \\ X_{\ell+1} \\ X_{I\bar{z}}
\end{bmatrix}
=
\begin{bmatrix}
\gamma_1 \\ \gamma_2 \\ \gamma_3 \\ \gamma_{\ell-1} \\ \gamma_\ell \\ \gamma_{\ell+1} \\ \gamma_{I\bar{z}}
\end{bmatrix}
$$

In the backsubstitution, we compute

$$X_{IZ} = Y_{IZ}$$

and $X_j = Y_j - \alpha_j X_{j+1} - \beta_j X_\ell$ for $j = IZM1, \ldots 1$

where $\beta_j = 0$ for $j > \ell - 2$

Since the γ, α, and β matrices are needed in the backsubstitution process, they are temporarily stored on a random access file and then recalled as needed. This was done because the size of these matrices prohibited storing them for all levels simultaneously. For example, at each level γ and α consist of $50 \times IY^2$ words and β of $10 \times IY$ words. One should note that in the back substitution process the perturbation v field was explicitly set to be zero on the side boundaries.

12. Model Inputs

In order to compute the response of the atmosphere to a specified heat input we must specify the following:

1) domain for model

2) zonal wavenumber, s

3) frequency σ, relative to the ground

4) damping rate, D

5) viscosity profiles, $\nu(Z)$ and $\hat{\nu}(Z)$

6) distribution of cumulus mass flux $\bar{M}_c (\theta, Z)$, and $M_c' (\theta, Z)$

7) basic state flow field $\bar{u}(\theta, Z)$, $\bar{v}(\theta, Z)$, and $\bar{w}(\theta, Z)$

8) mean temperature distribution $\bar{T}(\theta, Z)$

9) perturbation heating pattern $Q'(\theta, Z)$

10) coordinate stretching in vertical and latitudinal directions

13. Results

In our initial experiment, we sought to duplicate Holton's (1971) results by setting up our model with a motionless basic state and using the parameters and grid resolution similar to Holton's. To accomplish this we specified the following inputs.

1) The latitudinal domain for this experiment was from the equator to ~30°N with a resolution of approximately 2° in the tropics (i.e. IY=11). A rigid lid was placed at z=3 (~50mb) with a resolution $\Delta z=0.1$ (i.e. IZ=31). In addition, cloud base was placed at ~950 mb (z=0.1), whereas the tropopause was set at 135 mb (z=2.0).

2) The zonal wavenumber was set to s=10, corresponding to a zonal wavelength of ~4000 km.

3) The angular frequency was set to $\sigma = \Omega/5$days, corresponding to a westward propagation with a period of 5 days relative to the ground.

4) The dissipation coefficients (DISWIND and DISTEMP) were set to 0.03, which corresponds to damping time scale of 2.65 days for Rayleigh friction (α_r) and Newtonian cooling (α_N). In Holton's model the linear damping terms α_r and α_N were necessary to prevent the occurrence of singularities in the final diagnostic equation.

5) The viscosity profile was given by $\hat{\nu}(z)=\nu(z)=\begin{cases} 10^2 m^2 s^{-1} & z<z_c \\ \\ 1 m^2 s^{-1} & z \geq z_c \end{cases}$

6) Cumulus mass flux was set to $\bar{M}_c(\theta,z) = M'_c(\theta,z) = 0$

7) The components of the basic state flow field were set to $\bar{u}(\theta,z) = \bar{v}(\theta,z) = \bar{w}(\theta,z) = 0$.

8) In this experiment the mean temperature ($\bar{T}$) distribution was obtained from the vertical temperature structure (shown in Fig. 13.1) of the mean annual atmosphere at 15°N (U.S. Standard Atmosphere Supplements, 1966). At each vertical grid point, values of $\bar{T}$ were linearly interpolated from the sounding in Fig. 13.1. To be consistent with the assumption of a motionless basic state, the latitudinal variation of mean temperature (i.e., $\partial\bar{T}/\partial\theta$) was set to zero.

9) The perturbation heating (Holton, 1971) was given by:

$$Q'(\theta,Z) = Q_o \cdot \exp[-(\frac{\theta-\theta_o}{\theta_1})] \cdot \exp\ (\frac{ZD}{2})$$

$$\times \begin{cases} ZD/12 - \exp^{-ZD} & ZD < 12 \text{ km} \\ 7.-ZD/2. & 12 \le ZD \le 14 \text{ km} \\ 0. & ZD > 14 \text{ km} \end{cases}$$

where $ZD = z \times SH$
$SH \equiv$ scale height (8 km)

In the above equation ZD has the dimension of kilometers and Q_o is a constant chosen so that the vertically integrated heating rate at latitude θ_o is $\sim 3.6°K$ day^{-1}, which corresponds to a rainfall rate of 1 cm day^{-1}. In addition we have set $\theta_o = 8.63$, which corresponds to the latitude where the lateral heating distribution is a maximum, and $\theta_1 = 3.0$ (i.e. a half width of $\sim 3°$ latitude). A meridional plane cross section of the distribution of amplitude for the heat source is shown in Fig. 13.2. In Holton's paper, he states that the vertical distribution of condensation heating above 900 mb represents the large-scale heating of the atmosphere by deep cumulus convection, whereas the cooling near the lower boundary is thought to be primarily due to descent of low equivalent potential temperature air in downdrafts occurring in the rain areas.
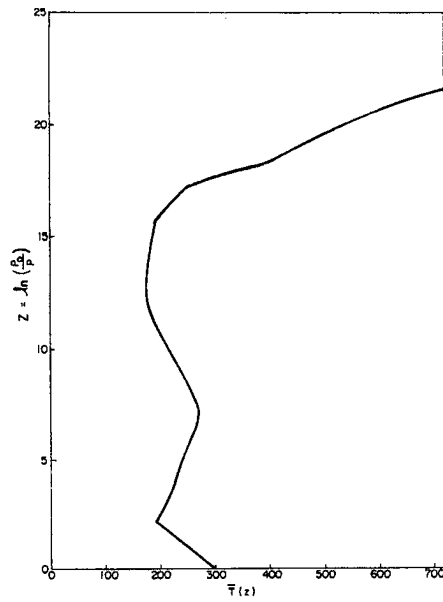
Fig. 13.1 Vertical temperature structure of the mean annual
atmosphere at 15°N (U.S. Standard Atmosphere Supplement, 1966).
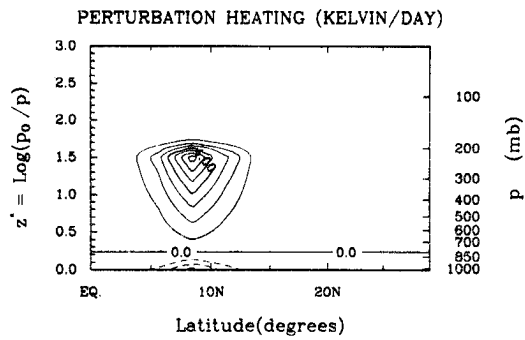
Fig. 13.2 A meridional plane cross section of the distribution of
amplitude of the perturbation heat source.

Fig. 13.3 shows the computed atmospheric response (as amplitude and phase) in the u, v, w, T, and Φ perturbation fields for the values of the parameters specified above. In addition to presenting the amplitude and phase of each field, we offer (Fig. 13.4) the reader a supplementary view of these fields by presenting their amplitudes at phase = 0° (where Q' is maximum) and at phase = 90° (one-quarter wavelength before maximum Q'). For the sake of comparison, Figs. 13.5 - 13.7 are shown here from Holton's (1971) paper depicting the atmospheric responses that were computed when he set the mean flow equal to zero in his model. One can readily verify that our results and Holton's are consistent for this experiment, providing some confidence that our model was properly formulated and coded.

Fig. 13.3 Computed atmospheric responses (amplitude and phase) in the u, v, w, T, and ϕ perturbation fields for Holton (1971) comparison run (solid lines positive values, dashed lines negative values). Phase is shown relative to heat source in Fig. 13.2.

(Fig. 13.3 on next page)

PERTURBATION U-VELOCITY (M/S)

PERTURBATION U-VELOCITY (PHASE)

PERTURBATION V-VELOCITY (M/S)

PERTURBATION V-VELOCITY (PHASE)

PERTURBATION W-VELOCITY (CM/S)

PERTURBATION W-VELOCITY (PHASE)

PERTURBATION TEMPERATURE (KELVIN)

PERTURBATION TEMPERATURE (PHASE)

PERTURBATION GEOPOTENTIAL (M^2/S^2)

PERTURBATION GEOPOTENTIAL (PHASE)

Fig. 13.4 Computed atmospheric responses (amplitude at phase = 0° and phase = 90°, where phase is relative to heat source in Fig. 13.3) in the u, v, w, T, and ϕ perturbation fields for Holton (1971) comparison run (solid lines positive values, dashed lines negative values).

(Fig. 13.4 on next page)

U'(M/S) AT PHASE = 0°

U'(M/S) AT PHASE = 90°

V'(M/S) AT PHASE = 0°

V'(M/S) AT PHASE = 90°

W'(CM/S) AT PHASE = 0°

W'(CM/S) AT PHASE = 90°

T'(KELVIN) AT PHASE = 0°

T'(KELVIN) AT PHASE = 90°

$\Phi'(M^2/S^2)$ AT PHASE = 0°

$\Phi'(M^2/S^2)$ AT PHASE = 90°
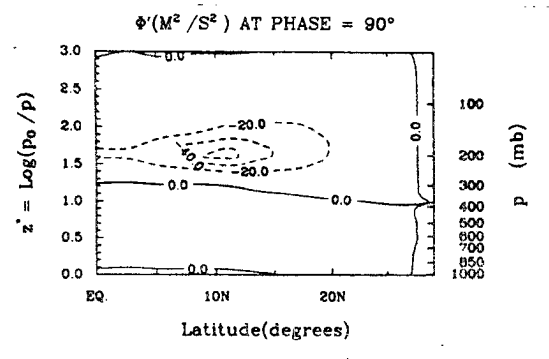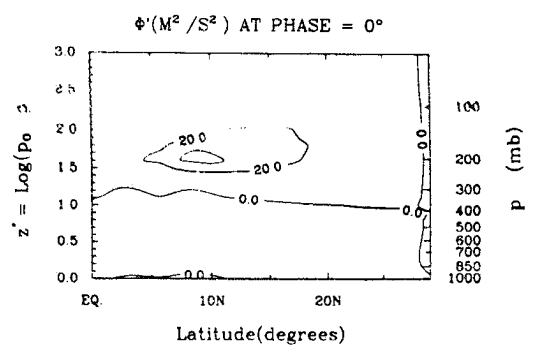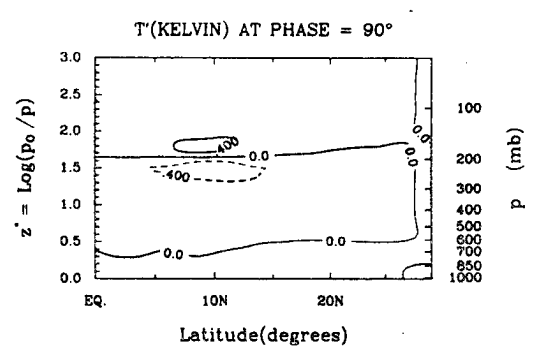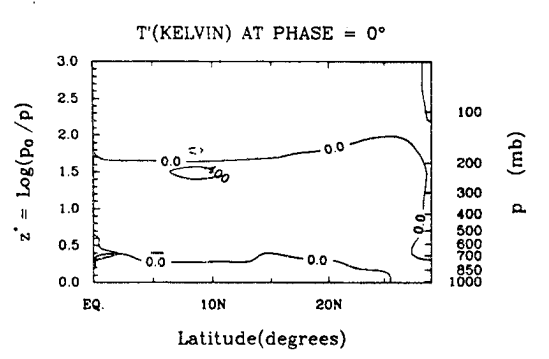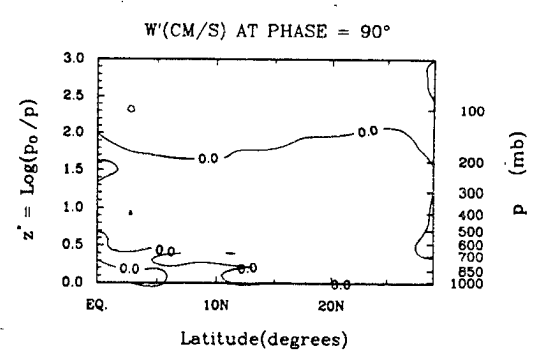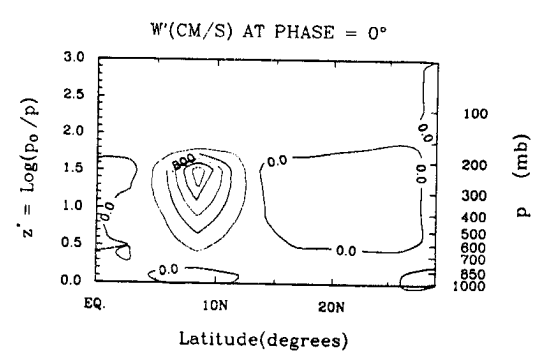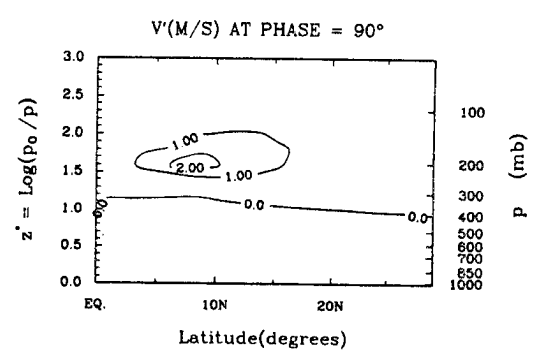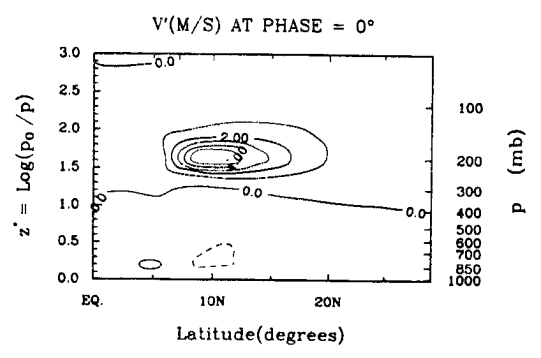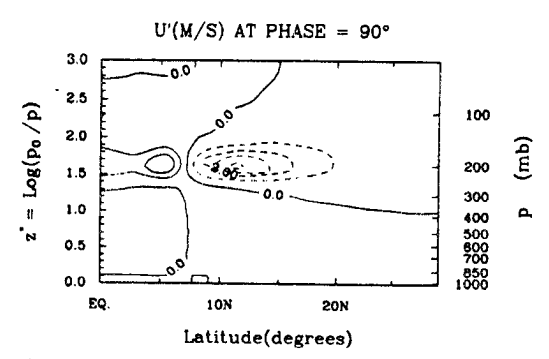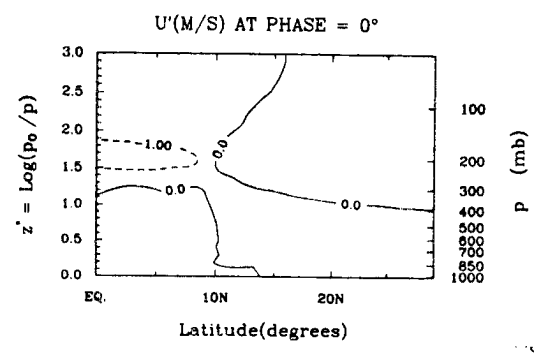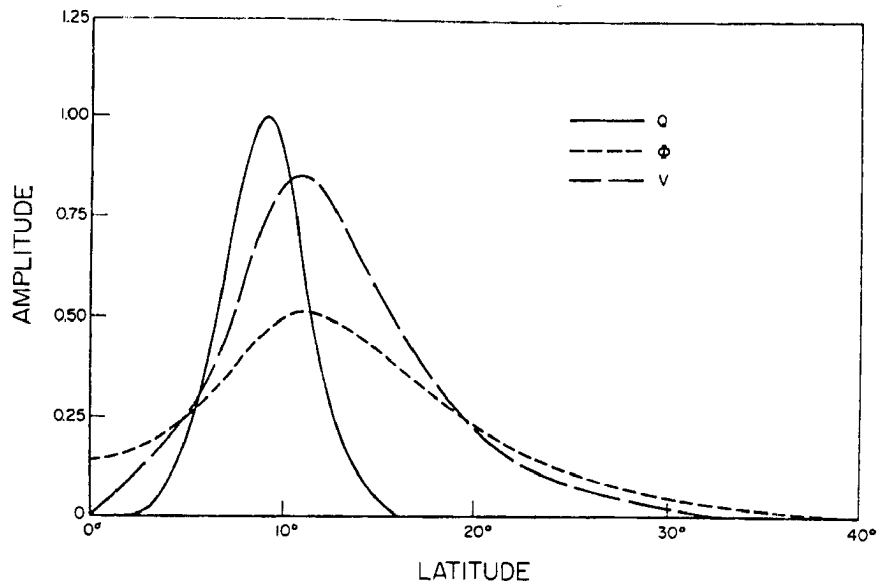
Fig. 13.5 Amplitude (non-dimensional) of the diabatic heating Q, geo-
potential perturbation φ, and meridional velocity v vs latitude
at a height of 13 km for case with no mean flow. Unit amplitude
corresponds to a heating rate of 4°C day$_{-1}$, a geopotential height
of 10 m^2 sec^{-2}, and a velocity of 10 m s^{-1} (from Holton, 1971).
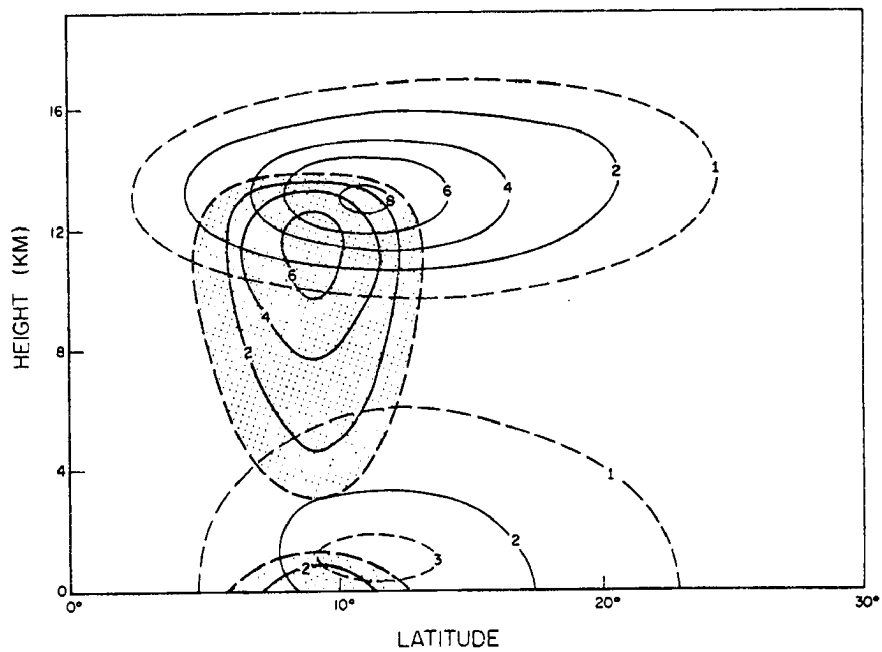
Fig. 13.6 Meridional cross section of the amplitude ($^\circ$C day^{-1}) of diabatic heating [heavy lines, shaded region] and the meridional velocity (m·sec^{-1}) [light lines] for case with no mean flow (from Holton, 1971).
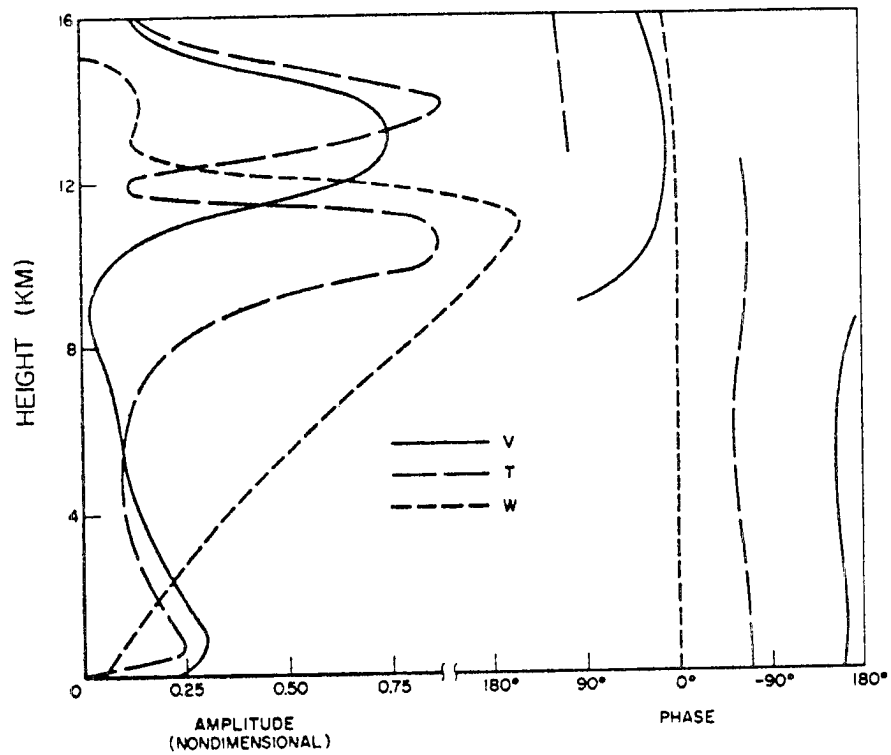
Fig. 13.7 Vertical profiles of amplitude and phase of meridional
velocity v, temperature perturbation T, and vertical velocity w
for case with no mean flow. Unit amplitude corresponds to
v = 10 m sec^{-1}, w = 2 cm sec^{-1}, T = 1°C. The phase is shown
relative to heat source (from Holton, 1971).

14. Optimization of Model on the CRAY-1 Computer

Being reasonably convinced that we had formulated our model correctly, we then sought to reduce its cost by optimizing the model's code (i.e., making the most efficient use of the architecture of the CRAY-1 system). This task was suggested by our need to increase the horizontal resolution of the model beyond 11 grid points; small increases in the number of points in the model's domain cause large increases in the computer resources that are used in the matrix inversion stage. For example, by increasing the number of horizontal nodes in the model from 11 to 15 points (see Table 1), the CRAY resources that are used increase by approximately 150%. Computer time is approximately proportional to IY^3.

The first step taken in optimizing our model was to time various sections of code. Through this process we determined that 95% of the execution time used in running the model was spent in subroutine LEQ2C. This library software routine written by IMSL was used to invert a full non-Hermitian complex matrix at each vertical level of the mode. The majority of the execution time spent within LEQ2C is used in obtaining a high accuracy solution which results from an iterative improvement scheme that uses double-precision arithmatic. With further testing as noted in Table 1, we were able to show that the iterative scheme as well as the double-precision arithmetic it utilizes are necessary in order for the solution produced by LEQ2C to converge. Although a compiled version of the IMSL software has recently been appended to the CRAY-1 library, the CRAY compiler is not able to vectorize the two recursive operations within the iterative improvement scheme which involves summing up a series of double precision numbers. With an optimized double-

55

precision adder, as SSUM is for single-precision numbers, we could envision a significant increase in the efficiency of LEQ2C and consequently our model.

As an alternative to using the time-consuming, yet highly accurate LEQ2C, we attempted the matrix inversions in our model with software from the LINPACK library. This software library was written for speed optimization on the CRAY-1 by referencing CRAY Assembly Language Basic Linear Algebra Subroutines (CAL BLAS). Surprisingly, use of the LINPACK software in our model resulted in the correct solution, in spite of the fact that only single precision arithmetic is used in the inversion routines. In addition, the execution time for running our model was reduced by 95% by using this efficient software! The computer runs referenced in this section are summarized in the following Table.

TABLE 1

DESCRIPTION	Results of RUN	CRAY-1 Resources Us (in CRAY hou
Standard run with 31 vertical levels and 11 horizontal nodes using LEQ2C matrix inverter	Correct results	.0396
Same as 1, except using LEQT1C matrix inverter (i.e. no iterative improvement scheme)	Erroneous results	.0018
Same as 1, except single precision arithmatic used in iterative improvement scheme in LEQ2C. This was accomplished by specifying OFF=P on the CFT card which at compile time causes all double-precision variables to be treated as real single-precision variables.	Interative improvement failed to converge. Erroneous results	.0074
Same as 1, except with 15 horizontal nodes	Correct results	.1002
Standard run with 15 horizontal nodes using LINPACK matrix inverter	Correct results	.0047

15. Computation of Basic State

As stated in the introduction of this paper, to better understand the structure and dynamics of tropical easterly waves, a model must incorporate a realistic basic state. In fact, the most important advance in our model design over previous attempts to simulate these weather systems is the explicit inclusion of a zonal ITCZ with associated vertical mass flux both on the cloud scale ($g\bar{M}_c$) and in the large-scale cloud environment ($\overline{pw}$). In the discussion that follows in this section, we describe a method for obtaining a a consistent basic state, given a specified $\bar{u}$ field.

15.1 Basic state equations

The equations for the basic state are given as follows:

Absolute Angular Momentum

$$\frac{\bar{v}}{a} \frac{\partial \overline{AM}}{\partial \theta} + \bar{w} \frac{\partial \overline{AM}}{\partial z} = a\cos\theta \bar{F}_u \qquad (15.1)$$

where: $\overline{AM} = a\cos\theta(\Omega a\cos\theta + \bar{u})$

$$\bar{F}_u = \frac{1}{p} \frac{\partial}{\partial z} [g\overline{M_c} (\bar{u} - \overline{u_c}) + g \frac{\mu\dagger}{H} \frac{\partial \bar{u}}{\partial z}] - \alpha_R \bar{u} + eddy\ terms$$

V-Momentum

$$\frac{\bar{u}^2}{a} \tan\theta + f\bar{u} + \frac{\partial \bar{\phi}}{a\partial\theta} = 0 \qquad (15.2)$$

Hydrostatic

$$\frac{\partial \bar{\phi}}{\partial z} = R\bar{T} \qquad (15.3)$$

58

Continuity

$$\frac{\partial(\bar{v}\cos\theta)}{a\cos\theta\partial\theta} + \frac{1}{\rho}\frac{\partial}{\partial z}(\rho\bar{w}) = 0 \tag{15.4}$$

Thermodynamic

$$\frac{\bar{v}}{a}\frac{\partial\bar{T}}{\partial\theta} + \bar{w}(\frac{\partial\bar{T}}{\partial z} + \kappa\bar{T}) = \frac{\bar{Q}}{c_p} + \frac{g}{\rho}\frac{\partial}{\partial z}\frac{\hat{\mu\dagger}}{H}\frac{\partial\bar{T}}{\partial z} - \alpha_N\bar{T} \tag{15.5}$$

In Eq. (15.1), $\overline{AM}$ represents the mean absolute angular momentum, whereas $a\cos\theta\bar{F}_u$ represents the sources of $\overline{AM}$. To arrive at the form of the v-momentum equation given here, we assumed that the difference of the mean v-component of forcing ($\bar{F}_v$) and advection of the mean meridional wind

$$(\frac{\bar{v}}{a}\frac{\partial\bar{v}}{\partial\theta} + \bar{w}\frac{\partial\bar{v}}{\partial z})$$

is small relative to the other terms in equation (15.2), and therefore can be neglected. Eq. (15.2) in this form represents gradient wind balance.

15.2 Computation of the $\bar{T}$ and $\bar{\Phi}$ fields

Differentiating Eq. (15.2) with respect to the vertical coordinate 'z' and applying Eq. (15.3) we obtain

$$\frac{\partial}{\partial z}(\frac{\bar{u}^2}{a}\tan\theta + f\bar{u}) = \frac{R}{a}\frac{\partial\bar{T}}{\partial\theta} \tag{15.6}$$

In this form Eq. (15.6) is the thermal wind equation which relates the vertical wind shear to the horizontal temperature gradient. From this equation and Eq. (15.2), one can note that at the equator (i.e., $\theta = 0°$) $\tan\theta = f = 0$, so that $\partial\bar{T}/\partial\theta = \partial\bar{\Phi}/\partial\theta = 0$. Furthermore by writing

$$\bar{T}(\theta,z) = T_0(z) + T_1(\theta,z) \tag{15.7}$$

$$\bar{\Phi}(\theta,z) = \Phi_0(z) + \Phi_1(\theta,z) \tag{15.8}$$

and defining $T_1(\theta=0,z) = 0$ which implies $\Phi_1(\theta=0,z) = 0$, it follows that

$$\bar{T}(0,z) = T_0(z)$$

$$\bar{\Phi}(0,z) = \Phi_0(z)$$

Using these definitions with the basic state equations, we are now able to compute the $\bar{T}(\theta,z)$ and $\bar{\Phi}(\theta,z)$ fields with the following procedure.

(1) Obtain $T_0(z)$ from a tropical sounding.

(2) Derive $\Phi_0(z)$ from $T_0(z)$ through the hydrostatic equation.

(3) Given $\bar{u}(\theta,z)$ as a prescribed input, compute $\bar{\Phi}(\theta,z)$ from the integral form of Eq. (15.2) shown below.

$$\bar{\Phi}(\theta,z) = \Phi_0(z) - a \int_0^\theta (\frac{\bar{u}^2}{a} \tan\theta + f\bar{u})d\theta \tag{15.9}$$

(4) Compute: $\Phi_1(\theta,z) = \bar{\Phi}(\theta,z) - \Phi_0(z)$

(5) Compute: $T_1(\theta,z) = \frac{1}{R} \frac{\partial \Phi_1(\theta,z)}{\partial z}$

(6) Compute: $\bar{T}(\theta,z) = T_0(z) + T_1(\theta,z)$

15.3 Computation of the $\bar{v}$ and $\bar{w}$ fields

Our goal has been to calculate a mean meridional circulation $(\bar{v},\bar{w})$ which is consistent with a specified mean zonal flow $\bar{u}$. In principal, the meridional circulation can be obtained from the angular momentum equation (15.1) and the conservation of mass equation (15.4). If the zonal flow $\bar{u}$ is specified as a function of latitude and height and if

the source term for angular momentum, $a\cos\theta\bar{F}_u$, is known **and** consistent, then $\bar{v}$ and $\bar{w}$ can be obtained in the following manner. First, we define a mean meridional streamfunction which satisfies (15.4):

$$ap\bar{w} = \frac{\partial\bar{\psi}}{\partial\mu}$$

$$pcos\theta\ \bar{v} = -\frac{\partial\bar{\psi}}{\partial z}$$

where $\mu \equiv \sin\theta$, $d\mu = \cos\theta d\theta$. Then conservation of angular momentum (15.1) can be re-written:

$$J(\bar{\psi},\overline{AM}) = \bar{F}_u apcos\theta \qquad\qquad (15.10)$$

where $J(\bar{\psi},\overline{AM}) \equiv \dfrac{\partial\bar{\psi}}{\partial\mu}\dfrac{\partial\overline{AM}}{\partial z} - \dfrac{\partial\bar{\psi}}{\partial z}\dfrac{\partial\overline{AM}}{\partial\mu}$ is the Jacobian. If $\bar{F}_u$ and $\overline{AM}$ are known, we planned to calculate the mean meridional streamfunction $\bar{\psi}$ from (15.10) and then $\bar{v}$, $\bar{w}$ from the auxiliary relations. If the domain is closed, with no mass flux through the boundaries, we can set $\bar{\psi}=0$ on all boundaries. Since a steady state is assumed, there can be no net source of angular domain: $\int \bar{F}_u a\cos\theta ad\theta Hdz = 0$.

Three different but related approaches have been used in our attempt to determine a realistic mean meridional circulation. They are outlined in the following subsections.

15.3.a First method

The source term $\bar{F}_u$ for mean zonal momentum was calculated from the equation following (15.1), neglecting all eddy terms. Thus the $\bar{M}_c$ and $\bar{u}$ fields were used in parameterizing the source. With finite differencing, an inhomogeneous set of linear equations for $\bar{\psi}$ at the grid points results. We attempted to solve this system of equations using standard matrix routines, but never achieved a useable solution for $\bar{\psi}$.

Part of the reason for this failure, we suspect, is that the problem is over-determined and a solution cannot be found. Specifically, the Jacobian contains only a first-order derivative in the vertical dimension, but two boundary conditions are prescribed ($\bar{\psi}=0$ at top and bottom).

15.3.b Second method

This method is a modification of the first, in which we retain the same approach using $\bar{F}_u$ but admit to some uncertainties in $\bar{F}_u$ near the upper and side boundaries. Specifically, $\bar{v}$ and $\bar{w}$ are obtained by integrating upward from the lower boundary and laterally between northern and southern boundaries. $\bar{v}$ is modified gradually in the vicinity of the side boundaries so that it vanishes at the side walls. $\overline{pw}$ is modified smoothly above the tropopause so that the vertical mass flux vanishes at the model top. In this way, conservation of mass is retained, while the momentum balance is altered slightly, in a sense by sources of unknown origin (e.g., eddy terms). These modifications in $\bar{v}$ and $\bar{w}$ occur far from the central region, so that the perturbation fields of interest are not significantly affected.

We write the continuity equation in the form

$$\frac{\partial \overline{pw}}{\partial z} = - \frac{\partial}{\partial \mu} \left(\frac{\overline{pv}}{a} \cos\theta \right), \tag{15.11}$$

and the angular momentum equation in the form

$$\frac{\overline{pv}}{a} \cos\theta = \frac{\bar{F}_u pa\cos\theta - \overline{pw} \frac{\overline{\partial AM}}{\partial z}}{\frac{\overline{\partial AM}}{\partial \mu}} \tag{15.12}$$

At the lower boundary $\bar{w}(z=0)=0$. Since any horizontal shear of the mean

zonal flow at the equator is eliminated by inertial instability

(Stevens, 1983), we assume $\partial\overline{AM}/\partial\mu=0$ at the equator.

The algorithm follows these steps.

(1) Given a specified $\bar{u}$ field, compute $\bar{F}_u$, $\overline{AM}$, $\partial\overline{AM}/\partial z$, and $\partial\overline{AM}/\partial\mu$ at
every point in the model's domain.

(2) Assuming $\bar{w}(z=0) = 0$, compute $\bar{v}$ at $z = 0$ using (15.12).

(3) Calculate $\overline{pw}$ at the next higher level 'j' by vertically integrating
Eq. (15.11) between a lower level 'j+1' and level 'j'.

(4) Compute $\overline{pv}/a$ at level 'j' by using (15.12) unless calculation
occurs at equator. At the equator $\partial\overline{AM}/\partial\mu = 0$ so that instead of
using (15.12), $\overline{pv}/a$ is interpolated from values of $\overline{pv}/a$ on either
side of the equator. If a side boundary lies on the equator (i.e.,
i=1 corresponds to θ=0) then $\overline{pv}/a$ at i=1 is extrapolated from
values of $\overline{pv}/a$ at i=2,3, and 4.

(5) Repeat steps '3' and '4' for all vertical levels.

(6) Since we know that $\overline{pw}$ is "small" high enough in the atmosphere, we
alter the $\bar{w}$ field above z=ZTROP so that it trails off smoothly to
zero at the top of the model.

(7) Alter the $\bar{v}$ field to maintain mass continuity in regions where the
$\bar{w}$ field was altered in step '6'. In addition, change $\bar{v}$ at the side
boundaries and adjacent points so that it trails off to zero on
these side borders.

In order to compute the $\bar{v}$ and $\bar{w}$ fields given the procedure listed above, $\bar{u}(\mu,z)$ and $\bar{M}_c(\mu,z)$ must be specified. To provide for conservation of angular momentum the following constraints were applied to the $\bar{u}$ field: (1) $\partial \bar{u}/\partial z = 0$ at the top of the model, and (2) the viscous flux of angular momentum must be zero when averaged over the lower boundary (i.e. $\int \frac{\partial}{\partial z} (\bar{u}a\cos\theta)d\mu=0$).

As an example, we show the mean meridional circulation obtained by this method with a prescribed $\bar{u}$ flow consisting of easterlies in the tropics and westerlies in the middle latitudes.

$$\bar{u}(\mu,z) = \text{(Easterly component)} + \text{(Westerly component)} \qquad (15.13)$$

where

Easterly component $\equiv$ U1 $\times$ F1 $\times$ G1

$$U1 = -5 \text{ m s}^{-1}$$

$$F1(\mu) = \frac{1.}{(1. + (\frac{\mu}{\mu_1})^2)} \quad : \quad \mu_1 = 0.2$$

$$G1(z) = 1. - \sin(\pi \times \frac{z}{6.}) \; , \; z \leq 3$$

Westerly component $\equiv$ U2 $\times$ F2 $\times$ G2

$$U2 = 15 \text{ m s}^{-1}$$

$$F2(\mu) = \begin{cases} 0 & \mu \leq \mu_2 \\ (\frac{\mu-\mu_2}{\mu_3})^2 & \mu > \mu_2 \end{cases} \quad : \quad \mu_2 = 0.2, \; \mu_3 = 0.3$$

$$G2(z) = 1. + \cos\left(\pi \times \frac{(3.-z)}{4.}\right) \; , \; z < 3$$

In our present calculation, the mean cumulus mass flux $\bar{M}_c$ profile is given by:

$$\bar{M}_c = \bar{M}_{co} \times \text{EXPON} \times \text{ZFUNC} \tag{15.14}$$

where

$\bar{M}_{co}$ = 5 mbars/hour (magnitude of deep cloud mass flux from Yanai et. al, 1973)

$$\text{EXPON} = \exp\left[-\left(\frac{\mu - \mu\phi}{\mu 1}\right)^2\right]: \quad \mu_o = 0.15, \quad \mu_1 = 0.10$$

$$\mu = \sin(\theta)$$

$$\text{ZFUNC} = \left(1 - \exp\left(\frac{PT - PRES}{PDRT}\right)\right)$$

$PT = e^{-ZTROP}$ (i.e. non-dimensional pressure at tropopause)

PDRT = 0.10 (i.e. vertical decay scale used to simulate the detrainment layer at cloud top)

$PRES = e^{-z}$

Once the $\bar{M}_c$ field is computed, a 7-point running average is applied to this field in the vicinity of the tropopause in order to smooth out the vertical discontinuity of $\bar{M}_c$ in this region. The distributions of $\bar{u}(\mu,z)$ and $\bar{M}_c(\mu,z)$, as expressed in Eqs. (15.13) and (15.14), are shown respectively in Figs. (15.1) and (15.2). The corresponding field of $\overline{AM}$ is shown in Fig. 15.3, whereas the source field $\bar{F}_u$, which is parameterized from $\bar{u}$ and $\bar{M}_c$, is shown in Fig. 15.4.

Using these $\bar{u}$ and $\bar{M}_c$ fields, the resulting mean meridional circulation is shown in Figs. 15.5 ($\bar{v}$) and 15.6 ($\bar{w}$). We see that in the ITCZ region of maximum cloud mass flux $\bar{M}_c$, the mean vertical velocity $\bar{w}$ is actually downward. Yanai et al. (1973) demonstrated that $\overline{pw}$ and $g\bar{M}_c$ are both upward and of comparable magnitude in the Inter-Tropical Convergence Zone (ITCZ); i.e., most of the vertical mass flux in the

MEAN U−VELOCITY (M/S)
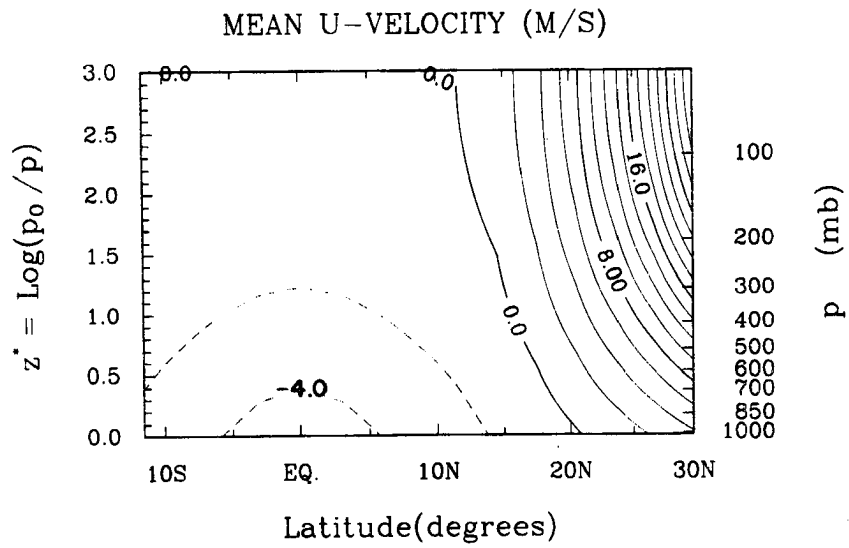
Fig. 15.1 Distribution of mean zonal wind ($\bar{u}$) in m·sec^{-1} (solid lines westerly wind, dashed lines easterly wind).

MEAN CUMULUS MASS FLUX (MB/HR)
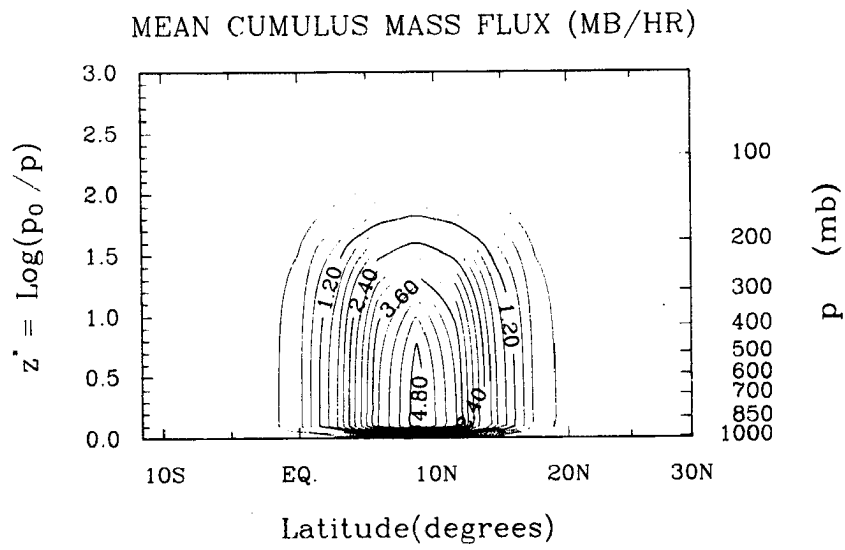
Fig. 15.2 Distribution of mean cloud mass flux ($\bar{M}_c$) in mb·hr^{-1} with off equatorial ITCZ.

ABSOLUTE ANGULAR MOMENTUM $(M^2/S) \cdot 10^{-8}$
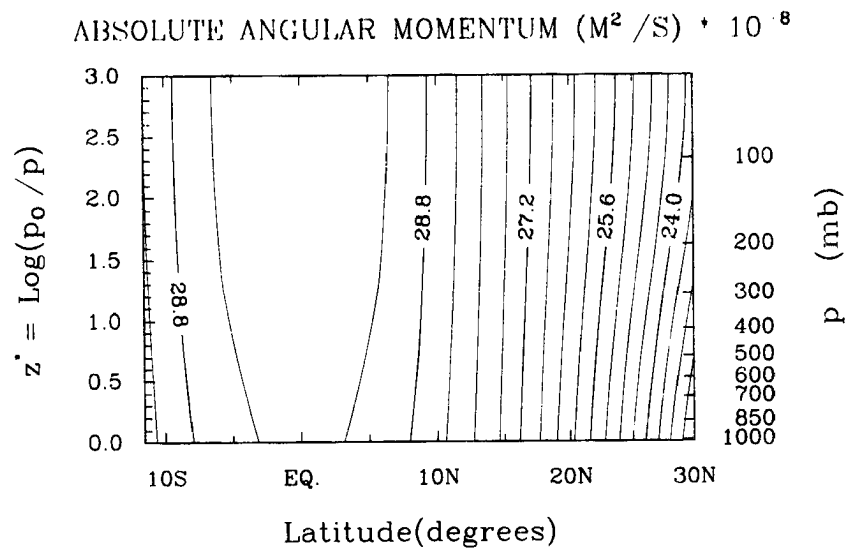
Fig. 15.3 Distribution of absolute angular momentum $(\overline{AM})$ in $m^2 \cdot s^{-1}$ $(\times 10^{-8})$.

ANGULAR MOMENTUM SOURCE (M^2 / S^2)
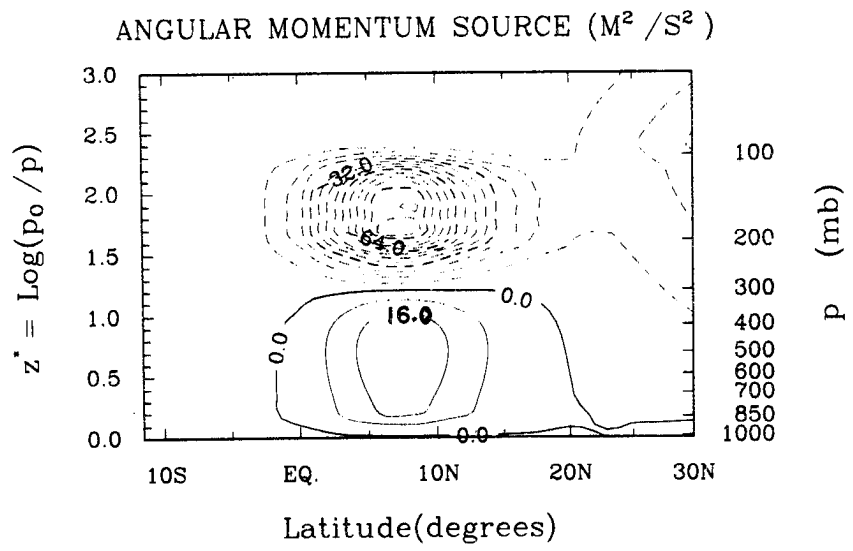
Fig. 15.4 Distribution of angular momentum source ($\bar{F}u$) in $m^2 \cdot s^{-2}$ with off-equatorial ITCZ (solid lines source region, negative lines sink region).

MEAN V-VELOCITY (M/S)
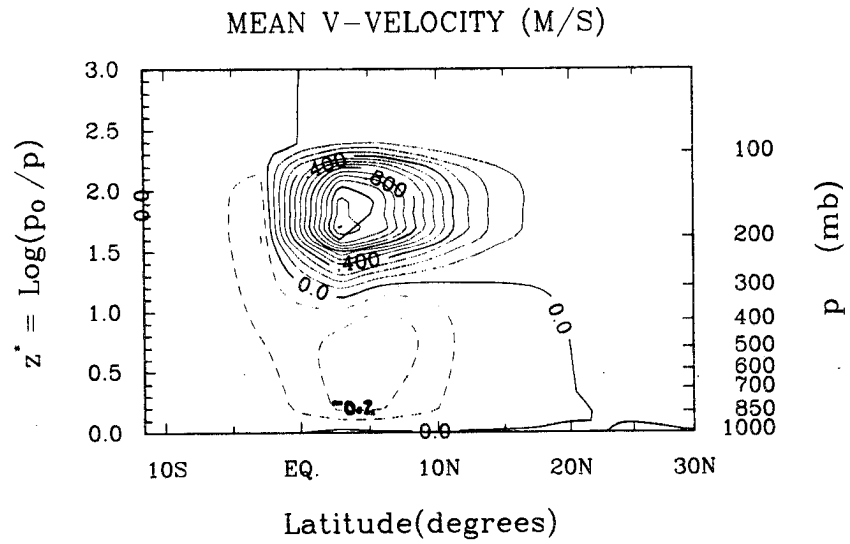
Fig. 15.5 Distribution of computed mean meridional velocity ($\bar{v}$) in m·sec^{-1} with off equatorial ITCZ (solid lines southerly wind, negative lines northerly wind).

MEAN W-VELOCITY (MBARS/HR)
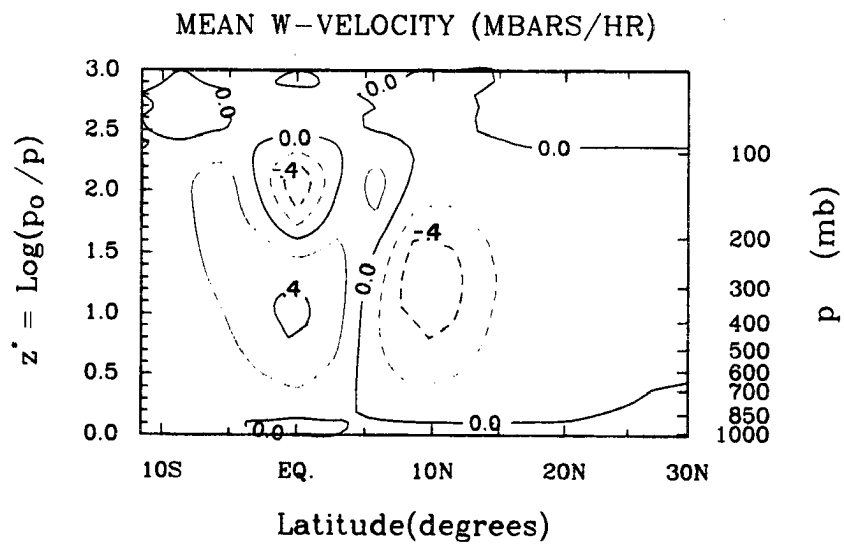
Fig. 15.6 Distribution of computed mean vertical velocity (w̄) in mb·hr⁻¹ with off equatorial ITCZ (solid lines upward motion, negative lines downward motion).

ITCZ takes place within the clouds. Because the observed cloud mass flux is slightly larger than $\overline{p}\overline{w}$, environmental subsidence between the clouds often results.

The results presented in Figs. 15.5 and 15.6 differ startlingly from the observations, in that the mean vertical mass flux in the ITCZ is <u>downward</u> and an order of magnitude smaller than the cloud mass flux. In the angular momentum budget, it is the horizontal advection and <u>not</u> the vertical advection that balances the cumulus source/sink term away from the equator. To examine why this balance occurs let us take the ratio of the vertical advection to the horizontal advection of angular momentum:

$$\frac{\overline{w}\,\frac{\partial \overline{AM}}{\partial z}}{\frac{\overline{v}}{a}\,\frac{\partial \overline{AM}}{\partial \theta}} = \frac{\frac{\partial \overline{\psi}}{\partial \mu}\,\frac{\partial \overline{AM}}{\partial z}}{-\frac{\partial \overline{\psi}}{\partial z}\,\frac{\partial \overline{AM}}{\partial \mu}}$$

Scaling the meridional flow as $\frac{\partial \overline{\psi}}{\partial z} \sim \frac{\overline{\psi}_o}{\Delta z}$; the vertical flow as $\frac{\partial \overline{\psi}}{\partial \mu} \sim \frac{\overline{\psi}_o}{\Delta \mu}$;

$\frac{\partial \overline{AM}}{\partial z} \equiv a\cos\theta \,\frac{\partial \overline{u}}{\partial z} \sim a\,\frac{\partial \overline{u}}{\partial z}$; $\frac{\partial \overline{AM}}{\partial \mu} \sim -a^2(2\Omega\sin\theta)$; we find:

$$\left|\frac{\text{Vertical Advection}}{\text{Horizontal Advection}}\right| \sim \frac{\Delta z}{\Delta \mu}\,\frac{\partial \overline{u}/\partial z}{2\Omega a \mu} \tag{15.15}$$

For the present calculation, we take $\Delta\mu \sim \mu \sim \mu_o = 0.15$, corresponding to the central latitude of the cloud mass flux distribution, $\Delta z \sim 1$ scale height,

$\frac{\partial \overline{u}}{\partial z} \sim \frac{\Delta \overline{u}}{\Delta z} \sim 5$ m·s^{-1} per scale height. Then the ratio of vertical to horizontal advection becomes

$$\left|\frac{\text{Vertical Advection}}{\text{Horizontal Advection}}\right| \sim \frac{1}{\mu_o{}^2} \cdot \frac{\Delta \overline{u}}{2\Omega a} \sim 0.2 \tag{15.16}$$

Hence horizontal advection dominates at the latitude of the ITCZ, while vertical advection must balance the source at the equator. For the same vertical shear $(\Delta\bar{u})$, the farther the ITCZ is away from the equator, the greater is the relative strength of the horizontal momentum advection.

With this dynamical balance, cloud mass flux and mean vertical motion are not comparable in an ITCZ away from the equator. Furthermore, downward mean motion generally occurs in the ITCZ to compensate the equatorial upward motion and thereby close the meridional cell.

For completeness, let us consider the case where the central latitude of the cloud mass flux is placed on the equator (see Fig. 15.7). The source of momentum $\bar{F}_u$, which corresponds to this distribution of $\bar{M}_c$ and the $\bar{u}$ field in Fig. 15.1, is shown in Fig. 15.8. Repeating the scaling argument given in Eq. (15.15) for this configeration of $\bar{M}_c$, we see that in this case vertical advection dominates at the latitude of the ITCZ. This is due to the fact that the denominator in Eq. (15.15) goes to zero, since $\mu \sim \mu_0 = 0$ in this case. The resulting mean meridional circulation shown in Figs. 15.9 (v) and 15.10 (w) is now consistent with Yanai's observations that $p\bar{w}$ and $g\bar{M}_c$ are both upward and of comparable magnitude in the ITCZ. For example, in the region of maximum $\bar{M}_c$ nearly 85% of the mean meridional circulation is accomplished by the cumulus mass flux.

This method represents a consistent dynamical framework for studying the mean meridional circulation. However, with an off equatorial momentum source this method fails to simulate the typical observations within the ITCZ.

15.3.c Third method

In the third approach, we again specify $\bar{u}$ and $\bar{M}_c$ empirically. In addition, we use a mean meridional circulation $(\bar{\psi})$ which is determined from observations. A consistent angular momentum source must then consist of the eddy terms as well as the explicit zonal-average quantities. We do not investigate the nature of these eddy terms, but assume their existence.

MEAN CUMULUS MASS FLUX (MB/HR)
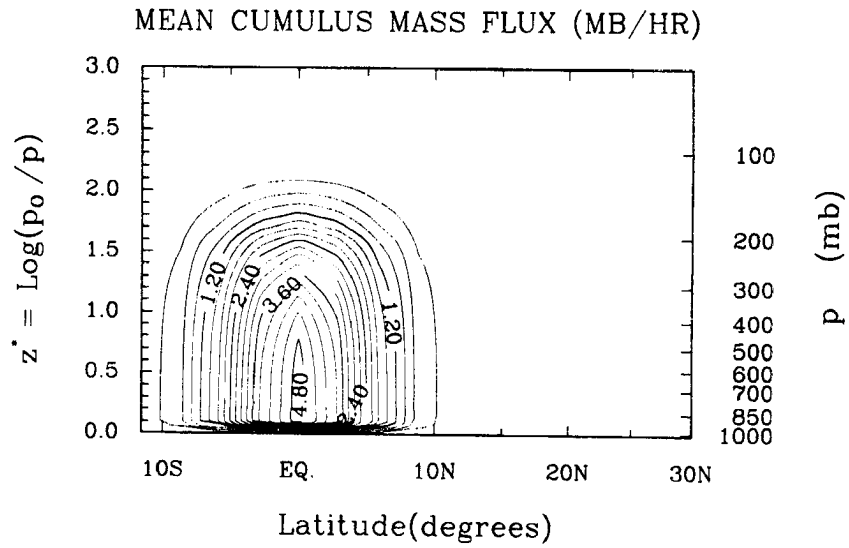
Fig. 15.7 Same as Fig. 15.2 except with ITCZ centered on equator.

ANGULAR MOMENTUM SOURCE (M^2/S^2)
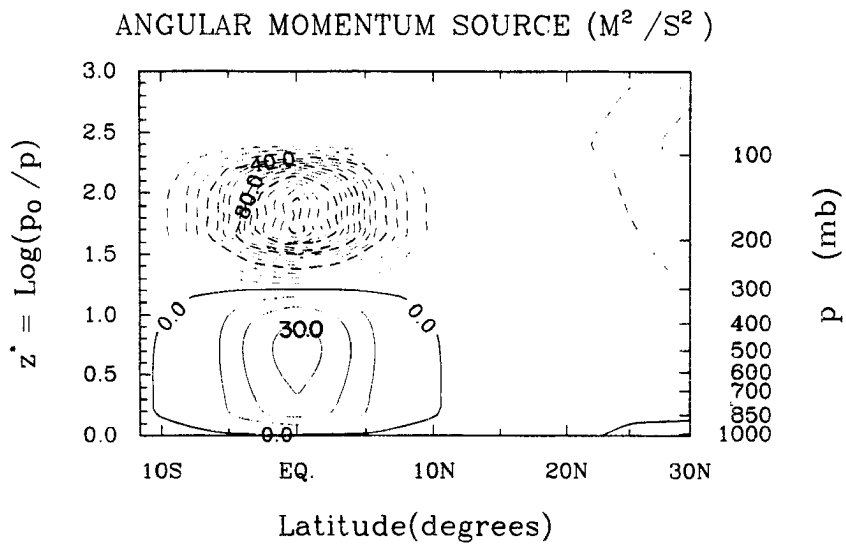
Fig. 15.8 Same as Fig. 15.4 except with ITCZ centered on equator.

MEAN V-VELOCITY (M/S)
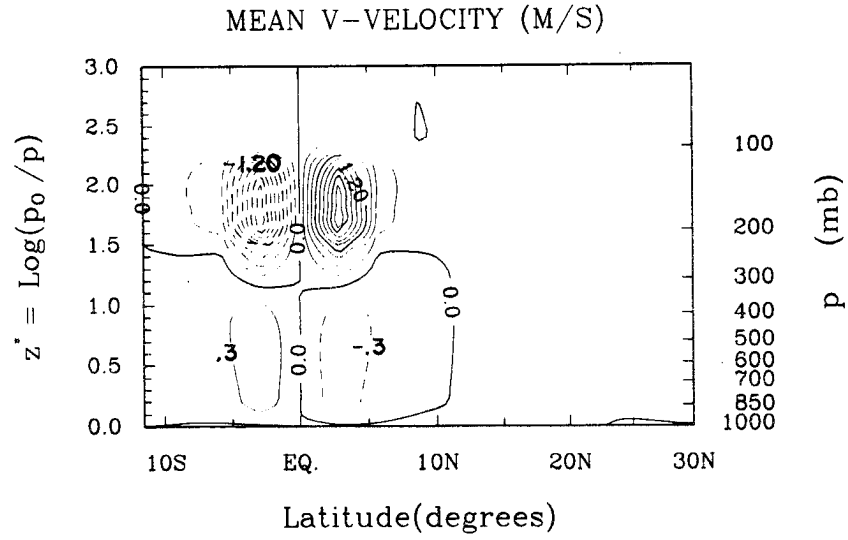
Fig. 15.9 Same as Fig. 15.5 except with ITCZ centered on equator.

MEAN W-VELOCITY (MBARS/HR)
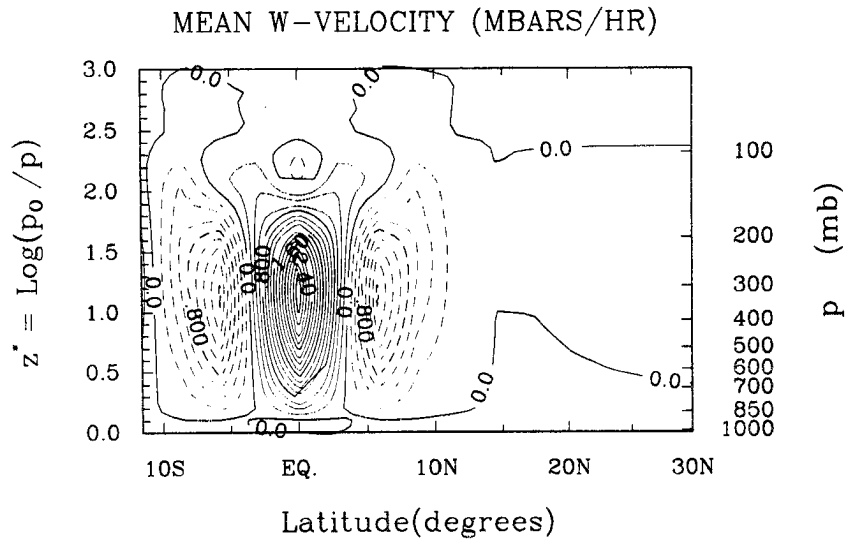
Fig. 15.10 Same as Fig. 15.6 except with ITCZ centered on equator.

16. Conclusions and Future Work

In summary, the characteristics unique to this model and/or important for applications include:

(a) The specifications of an "arbitrary" mean zonal flow which can depend on both latitude and height;

(b) Calculation of a mean meridional circulation which is dynamically consistent with the mean zonal flow (i.e., satisfies conservation of angular momentum, the balance approximation, the hydrostatic approximation, conservation of mass and energy);

(c) Vertical transport of momentum by the deep convective clouds in the tropics in both the mean and perturbation circulations;

(d) Spherical geometry;

(e) Coordinate stretching in both the vertical and latitudinal coordinates, which is represented in the coupled differential equations by finite differences;

(f) Very fine vertical grid resolution: experiments have been run with 31 points in the vertical; computer processing increases only linearly with the number of grid points in the vertical;

(g) Horizontal resolution of 15 to 20 points (square matrices with approximately five times the number of horizontal points must be inverted) at each vertical level;

(h) Very economic computation: the global response in a single zonal wavenumber with IY=21 and IZ=31 is obtained with approximately 13 seconds of NCAR CRAY time.

This linear model assumes that a frequency σ (which may be real, complex, or even zero) and a zonal wavenumber s is specified. In this way, response to a single Fourier component of forcing is studied. For

76

more general forcings, a Laplace transform in time and a Fourier transform in longitude is performed first; then this model calculates the complex response to each component. Finally, the various components are combined to obtain the actual response.

Now that the lengthy model development stage has come to a successful conclusion, we plan to apply our model to specific situations. The following discussion outlines a number of problems which we envision using our model on in the near future.

16.1 Tropical wave modeling

One of the problems to be addressed is the role and adequacy of Rayleigh friction as a parameterization of cumulus momentum transport in the tropics. Much of the recent work on the dynamics of planetary-scale tropical circulations have assumed this most simple parameterization of mechanical dissipation (e.g., Gill, 1980, Chang, 1977, and Chang and Lim, 1982). A comparison of such results with those with a more realistic parameterization is needed and can be accomplished in our model context.

It was hypothesized by Stevens et al., (1977) that cumulus momentum mixing is required to make temperature changes small in synoptic-scale, linear tropical waves. However, in our preliminary results shown by Stevens and Ciesielski (1982), it appears that the temperature changes are small (relative to diabatic heating and adiabatic cooling) with or without the inclusion of this physical process. Further investigation, at this point still preliminary, is indicating that another mechanism may be playing a more significant role in keeping the temperature changes small: namely, the existence of significant components of the response in modes with negative equivalent depths when the Doppler-

shifted period is on the order of days to weeks. These tentative con-clusions will become more concrete as the research progresses.

The sensitivity study of westward-propagating tropical disturbances to a zonal mean wind with realistic vertical and latitudinal shear is also planned. Specifically, wind regimes representative of the western Pacific and the eastern Atlantic will be considered in order to compare model wave structure and characteristics with the observed.

Finally, observational evidence from both GATE and MONEX is indi-cating that significant precipitation in tropical systems occurs in the mesoscale regime (Houze and Betts, 1981, and Johnson, 1982). This new information needs to be taken into account, for both mesoscale and convective scale condensation and precipitation influence the param-eterized diabatic heat source for the synoptic disturbance, whereas the convective scale vertical transport of horizontal momentum very likely dominates the mechanical forcing/dissipation of the synoptic scale by smaller scale systems. We intend to pursue the ramifications of the influence of these two smaller scales (not just the convective) on the synoptic systems.

16.2 Quasi-steady tropical circulations

Geisler (1981) has applied a model very similar to ours to the quasi-steady tropical east-west circulation known as the Walker cir-culation. However, the zonal mean flow was assumed to be negligible in that study and the effect of the mean meridional circulation on the disturbance was neglected. Although the latter may not have a signi-ficant effect, we expect the former to be rather crucial to the lati-tudinal extent of the circulation. In particular, the zero wind line is expected to play a rather important role in the Walker circulation. We

propose to investigate the Walker circulation in the context of this more realistic basic state.

Several recent studies (e.g., Webster, 1981, Hoskins and Karoly, 1981) have considered the influence of tropical heat sources with stationary planetary-scale midlatitude perturbations in linear model, with the purpose of explaining the interaction between tropics and midlatitudes on longer than synoptic time scales. This is a very exciting field that promises to increase the skill of long-range forecasting. In the linear wave theory, critical surfaces ($\bar{U} = c = 0$) strongly affect the propagation of energy from tropics to midlatitudes.

However, a paradoxical difference between the observations and the theory is present which we intend to address. Namely, observations over the past 25 years of synoptic-scale tropical systems have focussed on westward moving disturbances with typical propagation speeds around 5 ms^{-1}. If the _modulation_ of these systems is giving the quasi-steady heat sources assumed by the linear theories, then one would expect that the $\bar{U} = -5$ ms^{-1} surface would be an important factor, perhaps even more so than the zero wind surface, in the dynamics associated with the critical surface. This should be investigated and we propose to do so. Geisler and Stevens (1982) showed that very fine vertical resolution is required to represent these propagating modes.

Finally, further work needs to be done on the relative roles of heat sources and mechanical orographic forcing in the tropical/ midlatitude interaction problem. The linear, spherical, primitive equation model with high vertical resolution is a useful tool for this problem. We plan to exploit this developed tool in studying this important problem.

References

Albrecht, B. and S.K. Cox, 1975: The large-scale response of the tropical atmosphere to cloud-modulated infrared heating. _J. Atmos. Sci._, _32_, 16-24.

Chang, C.P., 1977: Viscous internal gravity waves and low-frequency oscillations in the tropics. _J. Atmos. Sci._, _34_, 901-910.

Chang, C.P. and H. Lim, 1982: On the effects of viscous damping on equatorial Rossby waves. _J. Atmos. Sci._, _39_, 1726-1733.

Geisler, J.E., 1981: A linear model of the Walker circulation. _J. Atmos. Sci._, _38_, 1390-1400.

Geisler, J.E. and D.E. Stevens, 1982: On the vertical structure of damped steady circulation in the tropics. _Quart. J. R. Met. Soc._, _108_, 87-93.

Gill, A.E., 1980: Some simple solutions for heat-induced tropical circulation. _Quart. J. Roy. Meteor. Soc._, _106_, 447-462.

Holton, J.R., 1971: A diagnostic model for equatorial wave disturbances: The role of vertical shear of the mean zonal wind. _J. Atmos. Sci._, _28_, 55-64.

Holton, J.R., 1975: The dynamic meteorology of the stratosphere and mesosphere. _Meteor. Monogr._, No. 37, Amer. Meteor. Soc., 56-57.

Hoskins, B.J., and D.J. Karoly, 1981: The steady linear response of a spherical atmosphere to thermal and orographic forcing. _J. Atmos. Sci._, _38_, 1179-1196.

Houze, R.A. and A.K. Betts, 1981: Convection in GATE. _Rev. Geophys. Space Phys._, _19_, 541-576.

Johnson, R.H., 1982: Vertical motion in near-equatorial winter monsoon convection. _J. Met. Soc. Japan_, _60_, 682-690.

Lindzen, R.S., and H.O. Kuo, 1969: A reliable method for the numerical integration of a large class of ordinary and partial differential equations. _Mon. Wea. Rev._, _97_, 732-734.

Mass, C., 1979: A linear primitive equation model of African wave disturbances. _J. Atmos. Sci._, _36_, 2075-2092.

Reed, R.J. and R.H. Johnson, 1974: Diagnosis of cloud-population properties in tropical easterly waves. Preprints Int. Tropical Meteorology Meeting, Nairobi, Kenya. Am. Meteoral. Soc., Part II, pp. 50-56.

Reed, R.J. and E.E. Recker, 1971:   Structure and properties of synoptic-scale wave disturbances in the equatorial western Pacific.   J. Atmos. Sci., 28, 1117-1133.

Schneider, E.K., 1977:   Axially symmetric steady state models of the basic for instability and climate studies, II.   Nonlinear calculations.   J. Atmos. Sci., 34, 280-296.

Schneider, E.K., and R.S. Lindzen, 1976:   A discussion of the parameterization of momentum exchange by cumulus convection.   J. Geophys. Res., 81, 3158-3160.

Schneider, E.K. and R.S. Lindzen, 1977:   Axially symmetric steady state models of the basic state for instability and climate studies, I.   Linearized calculations.   J. Atmos. Sci., 34, 263-279.

Shapiro, L.J., 1978:   The vorticity budget of a composite African tropical wave disturbance.   Mon. Wea. Rev., 106, 806-817.

Shapiro, L.J. and D.E. Stevens: Parameterization of convective effects on the momentum and vorticity budgets of synoptic-scale Atlantic tropical waves.   Mon. Wea. Rev., 108, 1816-1826.

Stevens, D.E., 1979:   Vorticity, momentum and divergence budgets of synoptic-scale wave disturbances in the tropical Eastern Atlantic.   Mon. Wea. Rev., 107, 535-550.

Stevens, D.E. 1983:   On symmetric stability and instability of zonal mean flows near the equator.   J. Atmos. Sci., 40, 882-893.

Stevens, D.E. and P. Ciesielski, 1982:   Transient disturbances in a linear model with an explicit Hadley circulation.   14th Technical Conference on Hurricanes and Tropical Meteorology, June 7-11, 1982, San Diego, CA.

Stevens, D.E. and R.S. Lindzen, 1978:   Tropical wave-CISK with a moisture budget and cumulus friction.   J. Atmos. Sci., 35, 940-961.

Stevens, D.E. and R.S. Lindzen and L.J. Shapiro, 1977:   A new model of tropical waves incorporating momentum mixing by cumulus convection.   Dyn. Atmos. Oceans, 1, 365-425.

Thompson, R.M., Jr., S.W. Payne, E.E. Recker and R.J. Reed, 1979:   Structure and properties of synoptic-scale wave disturbances in the intertropical convergence zone of the eastern Atlantic.   J. Atmos. Sci., 36, 53-72.

U.S. Standard Atmosphere Supplements, 1966,   U.S. Government Printing Office, Washington, DC.

Webster, P.J., 1981: Mechanisms determining the atmospheric response to sea surface temperature anomalies. J. Atmos. Sci., 38, 554-571.

Yanai, M., S. Esbensen and J.-H. Chu, 1973: Determination of bulk properties of tropical cloud clusters from large-scale heat and moisture budgets. J. Atmos. Sci., 30, 611-627.

Appendix

Flow Chart of the Fortran-coded Algorithms

This appendix provides flow charts of the computer code needed to run the model described in this paper. The code for running this model is divided into the following programs: GENVAR, GENCOEF, and DESRUN.

```
┌─────────────────────────────────────────────────────────────┐
│                          GENVAR                              │
│                                                              │
│  This program sets up the basic state, specifies all constants│
│                                                              │
│  to be used in the model, and prescribes the perturbation heating│
│                                                              │
│  function.                                                   │
└─────────────────────────────────────────────────────────────┘
                              │
                              ▼
┌─────────────────────────────────────────────────────────────┐
│                          GENCOEF                             │
│                                                              │
│  Using the output from 'GENVAR', this program generates the  │
│                                                              │
│  coefficients (see Section 7) which operate upon the non-    │
│                                                              │
│  dimensional dependent variables.                            │
└─────────────────────────────────────────────────────────────┘
                              │
                              ▼
┌─────────────────────────────────────────────────────────────┐
│                          DESRUN                              │
│                                                              │
│  Using coefficients generated in 'GENCOEF', this program sets│
│                                                              │
│  up the system AX=B, where X represents the five perturbation│
│                                                              │
│  variables at all grid points.  X is solved by using Lindzen │
│                                                              │
│  Kuo Gaussian Elimination.                                   │
└─────────────────────────────────────────────────────────────┘
```

A fourth program (PLOTSOL) provides contour plots of the solutions from the output of DESRUN and of the basic state fields from GENVAR.

A.   Program GENVAR

This program sets up the basic state, specifies all constants used in the model, and prescribes the perturbation heating function.

```
                        ┌─────────┐
                       (   START   )
                        └─────────┘
                             │
                             ▼
                    ┌──────────────────┐
                    │ SPECIFY CONSTANTS │
                    └──────────────────┘
                             │
                             ▼
            ┌──────────────────────────────────────────┐
            │ GENERATE HORIZONTAL AND VERTICAL COORDINATES │
            └──────────────────────────────────────────┘
                             │
                             ▼
          ┌──────────────────────────────────────────────┐
          │ COMPUTE FIELDS OF NON-DIMENSIONAL PRESSURE AND │
          │            THE CORIOLIS PARAMETER             │
          └──────────────────────────────────────────────┘
                             │
                             ▼
              ┌────────────────────────────────┐
              │ COMPUTE BASIC STATE VARIABLES   │
              └────────────────────────────────┘
                             │
                             ▼
     ┌────────────────────────────────────────────────────────┐
     │ SPECIFY PERTURBATION MASS FLUX AND PERTURBATION HEATING │
     └────────────────────────────────────────────────────────┘
                             │
                             ▼
          ┌──────────────────────────────────────────┐
          │ COMPUTE WAVENUMBER AT EACH MODEL LATITUDE │
          └──────────────────────────────────────────┘
                             │
                             ▼
              ┌────────────────────────────┐
              │ WRITE OUT REVELANT DATA     │
              └────────────────────────────┘
                             │
                             ▼
                        ┌─────────┐
                       (   STOP    )
                        └─────────┘
```
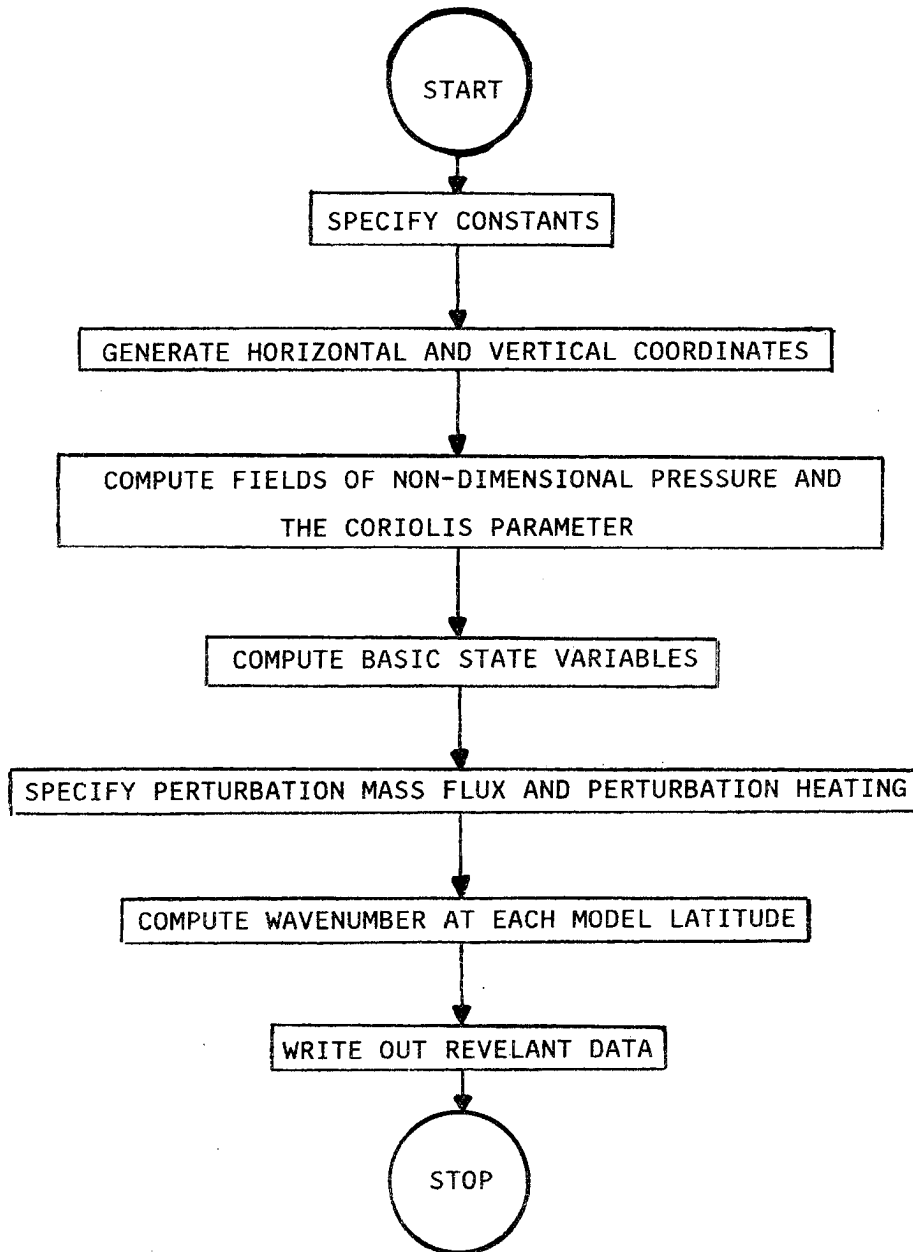
B.   Program GENCOEF

Using the output from 'GENVAR', this program generates the coefficients (see Section 7), which operate upon the non-dimensional dependent variables.

START

READ IN DATA GENERATED BY 'GENVAR' FROM A FILE

TRANSFER REVELANT DATA NEEDED BY 'DESRUN' TO COMMON BLOCK

COMPUTE COEFFICIENTS

ESTABLISH BOUNDARY CONDITIONS FOR z=0

WRITE OUT COEFFICIENTS AND OTHER PERTINENT DATA TO A FILE

STOP
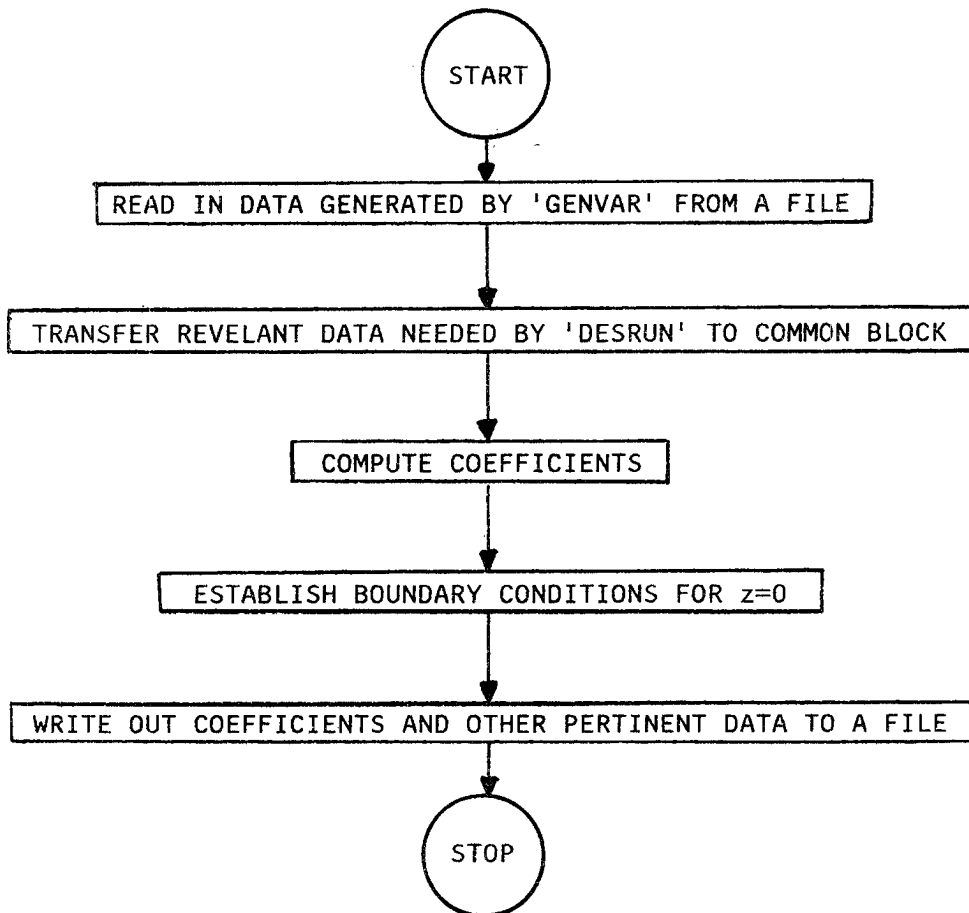
C. Program DESRUN

Using coefficients generated in 'GENCOEF', this program sets up the system AX=B, where X represents the five perturbation variables at all grid points. X is solved by using Lindzen Kuo Gaussian Elimination.

```
                          ┌─────────┐
                          │  START  │
                          └─────────┘
                               │
        ┌──────────────────────────────────────────────┐
        │  READ IN COEFFICIENTS AND OTHER PERTINENT DATA │
        │     GENERATED BY ' GENCOEF' FROM A FILE        │
        └──────────────────────────────────────────────┘
                               │
                        ┌──────────────┐
                        │  K = 1, IZ   │
                        └──────────────┘
                               │
                    ┌────────────────────┐
                    │ FILL IN SUB-MATRICES │
                    └────────────────────┘
                               │
        ┌──────────────────────────────────────────────┐
        │  MANIPULATE THE VARIOUS MATRICES TO ACCOUNT    │
        │          FOR SIDE BOUNDARY CONDITIONS          │
        └──────────────────────────────────────────────┘
                               │
        ┌──────────────────────────────────────────────┐
        │  SUB-MATRICES ARE USED TO FILL LARGER MATRICES │
        │   WHICH COMPRISE COEFFICIENT MATRIX 'A' AND     │
        │         RIGHT HAND SIDE MATRIX 'B'             │
        └──────────────────────────────────────────────┘
                               │
        ┌──────────────────────────────────────────────┐
        │  REDUCE SYSTEM TO AN UPPER TRIANGULAR MATRIX   │
        └──────────────────────────────────────────────┘
                               │
        ┌──────────────────────────────────────────────┐
        │  BACK-SUBSTITUTION FOR BOTTOM TWO LEVELS OF MODEL │
        └──────────────────────────────────────────────┘
                               │
        ┌──────────────────────────────────────────────┐
        │  LINDZEN-KUO BACKSUBSTITUTION FOR OTHER LEVELS │
        └──────────────────────────────────────────────┘
                               │
        ┌──────────────────────────────────────────────┐
        │  PRINT OUT SOLUTION AS AMPLITUDE AND PHASE     │
        └──────────────────────────────────────────────┘
                               │
               ┌────────────────────────────┐
               │  WRITE SOLUTION TO A FILE   │
               └────────────────────────────┘
                               │
                          ┌─────────┐
                          │  STOP   │
                          └─────────┘
```